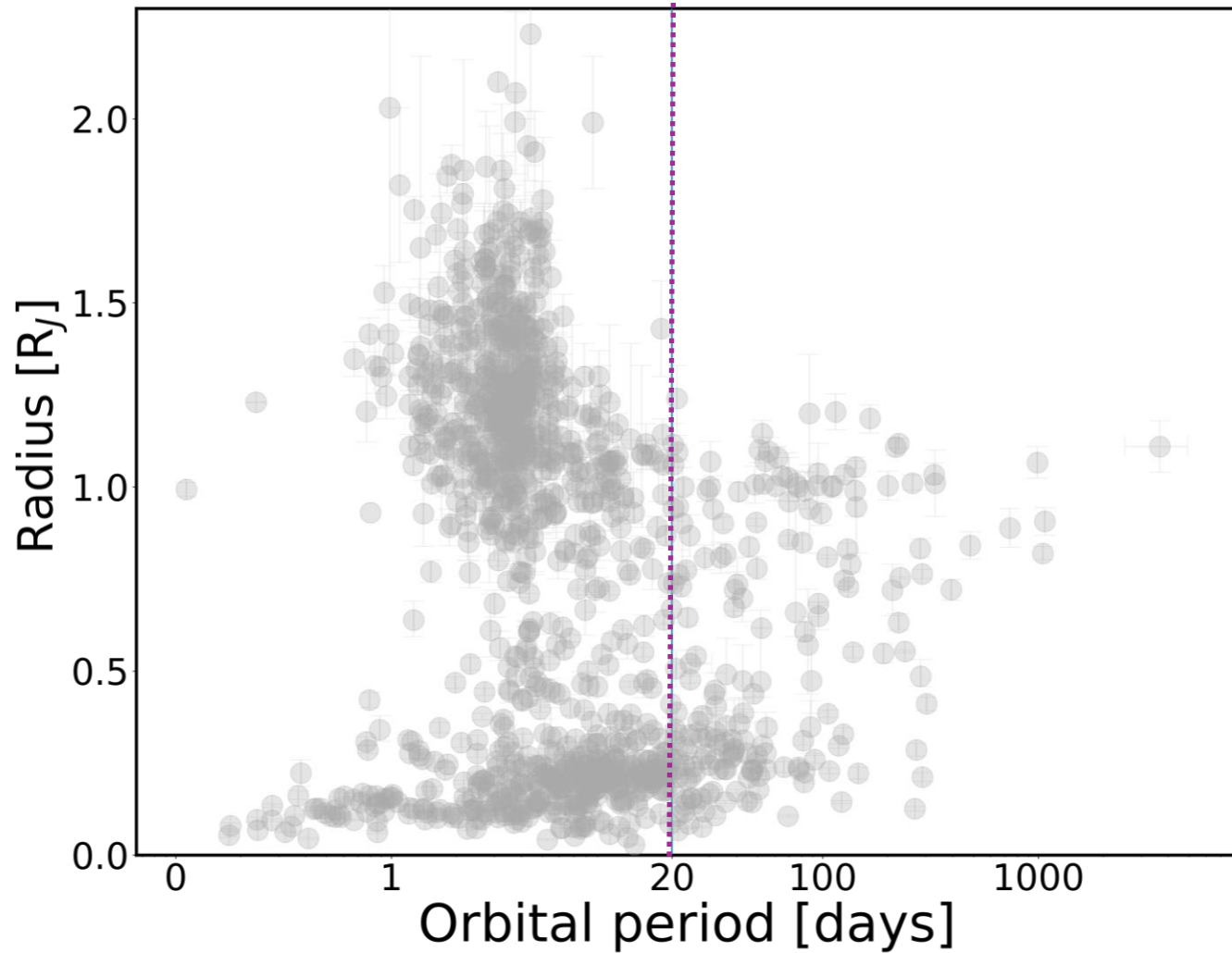




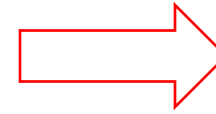
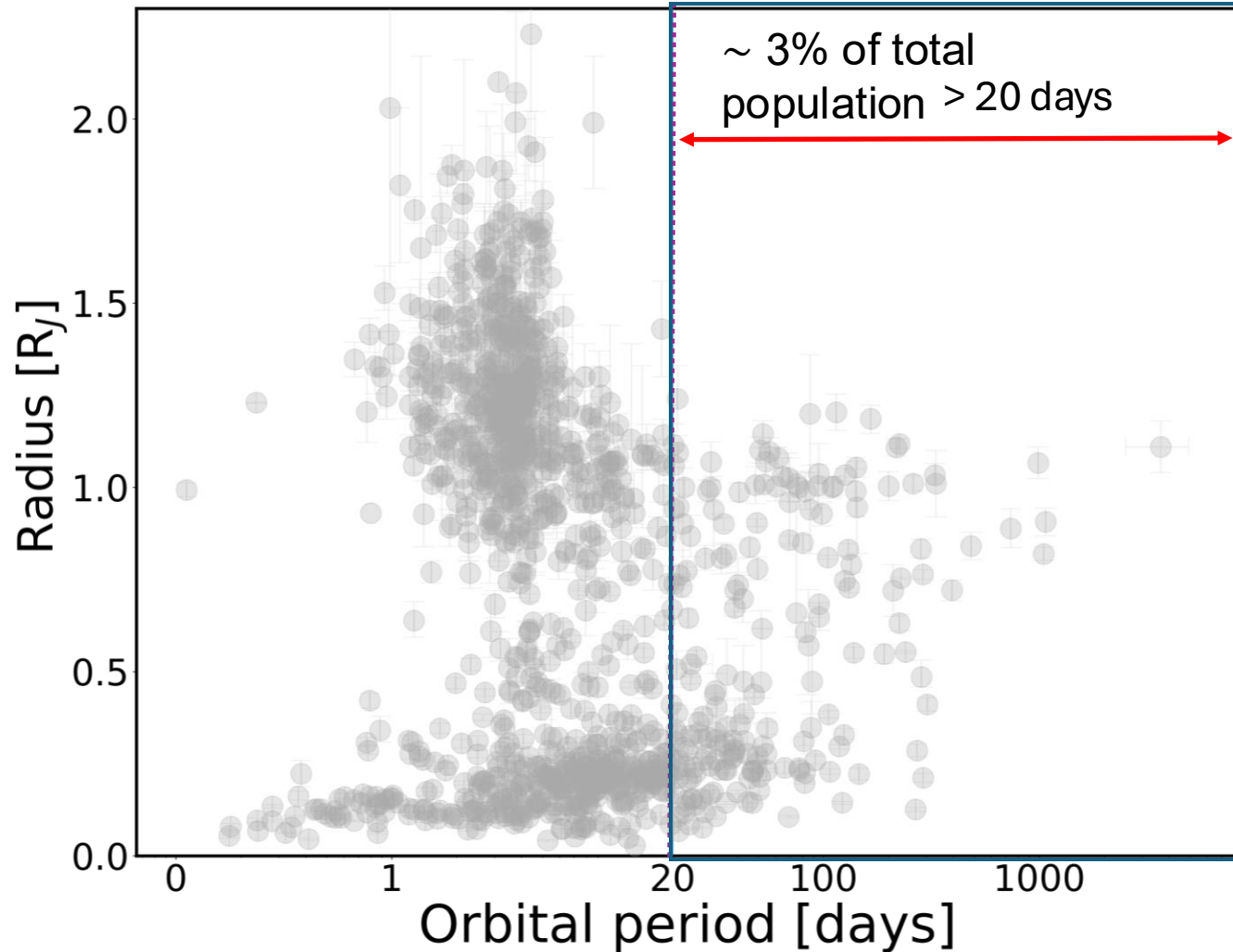
SOPHIE-TESS: Characterization of transiting warm Jupiters

N. Heidari, G. Hébrard, E. Martioli, F. Kiefer, A.C.M. Correia, X. Delfosse, I. Boisse, J. D. Eastman, J.M. Jackson, SOPHIE team, TESS team, et al.

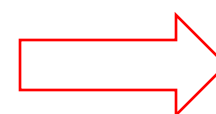
Institut d'Astrophysique de Paris (IAP),
July 2025



Orbital period versus planet radius of known exoplanets from NASA archival data (June, 2025) with accurate mass and radius better than 30 % .

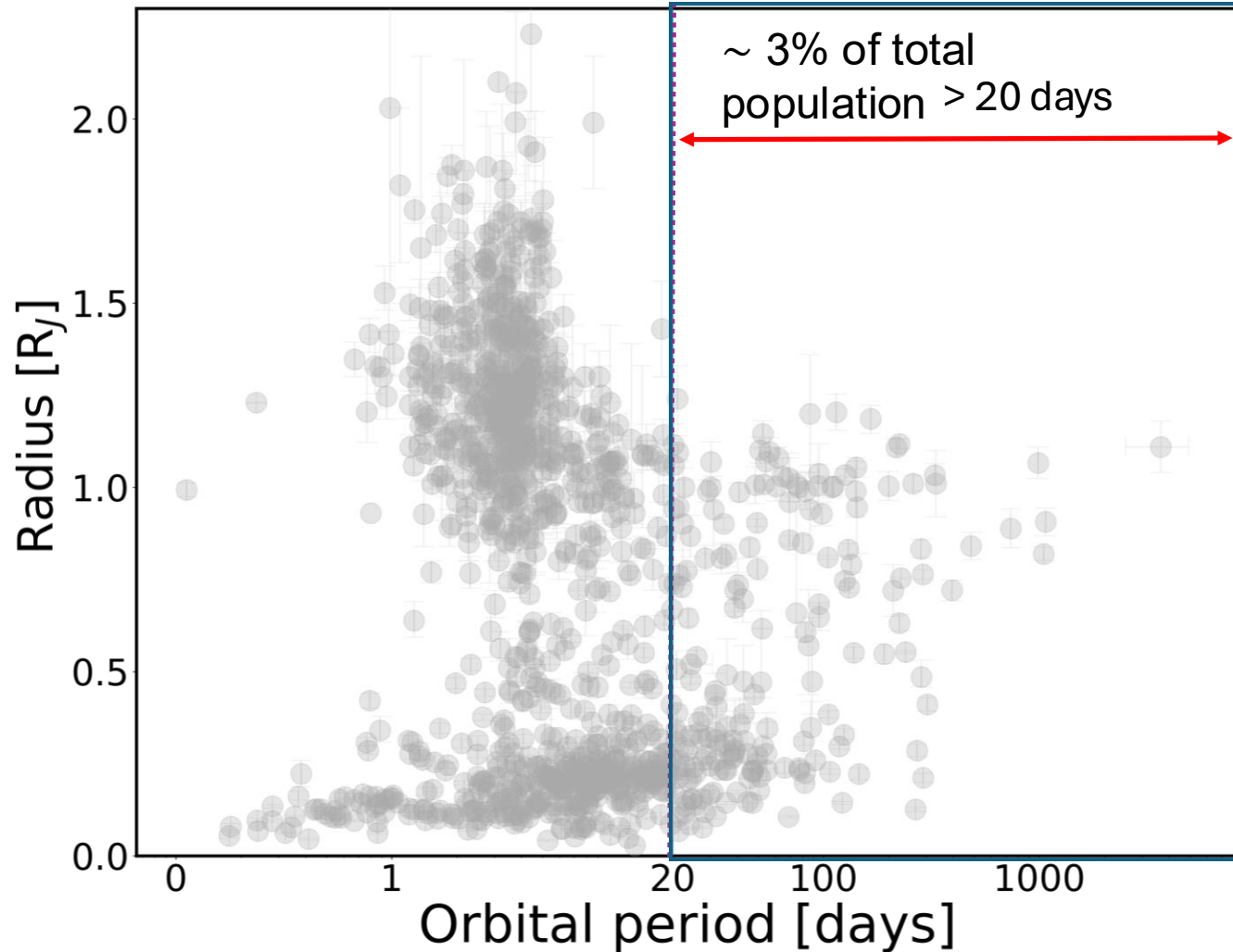


RV method requires measurements over extended time spans .



Transit method faces challenges due to both a lower transit probability and the limited baseline observations.

Orbital period versus planet radius of known exoplanets from NASA archival data (June, 2025) with accurate mass and radius better than 30 % .

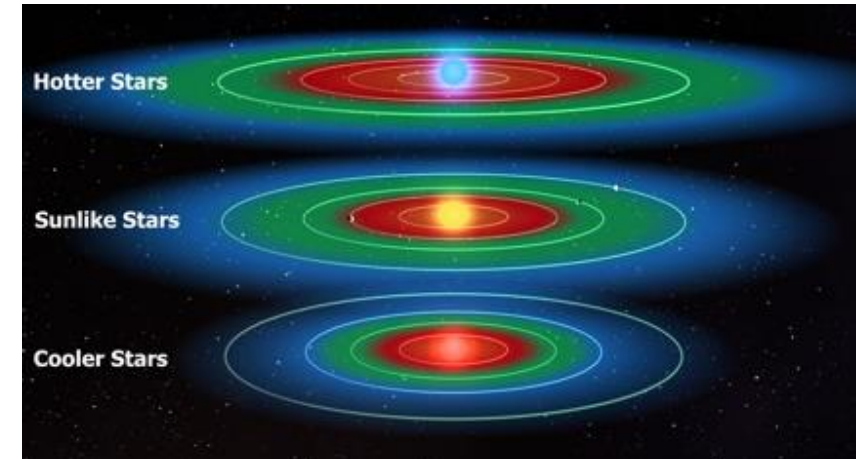
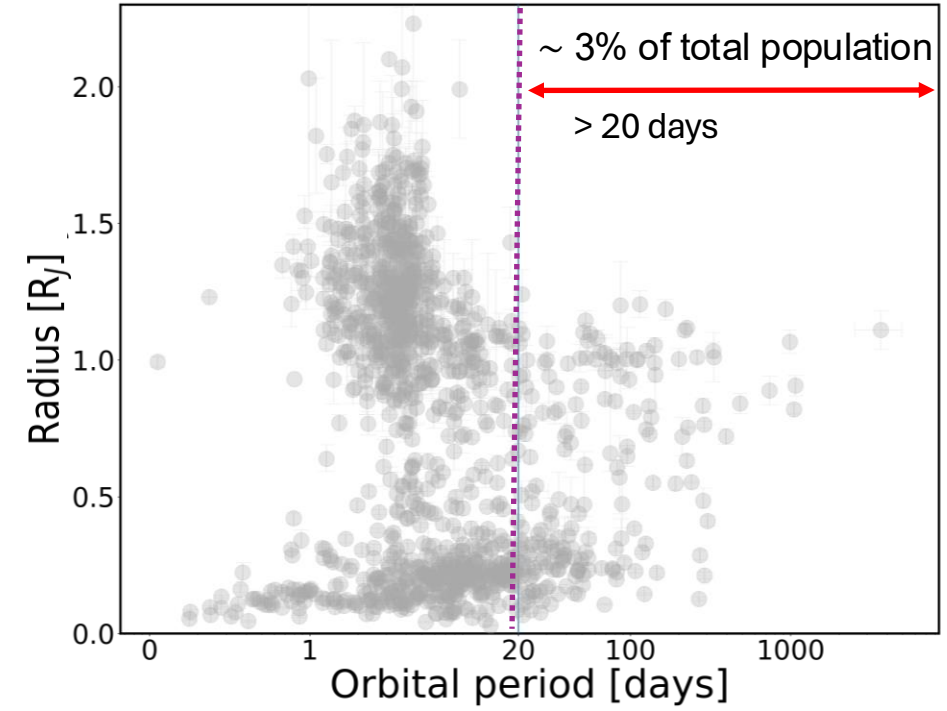


Systematic efforts should be dedicated to detecting and characterizing long-period planets.

Orbital period versus planet radius of known exoplanets from NASA archival data (June, 2025) with accurate mass and radius better than 30 % .

Why long-period planets are interesting?

- **Probe planets in the habitable zone**, as habitable zone around approximately M4/earlier spectral type stars is longer than ~ 11 days (Kopparapu+, 2013).

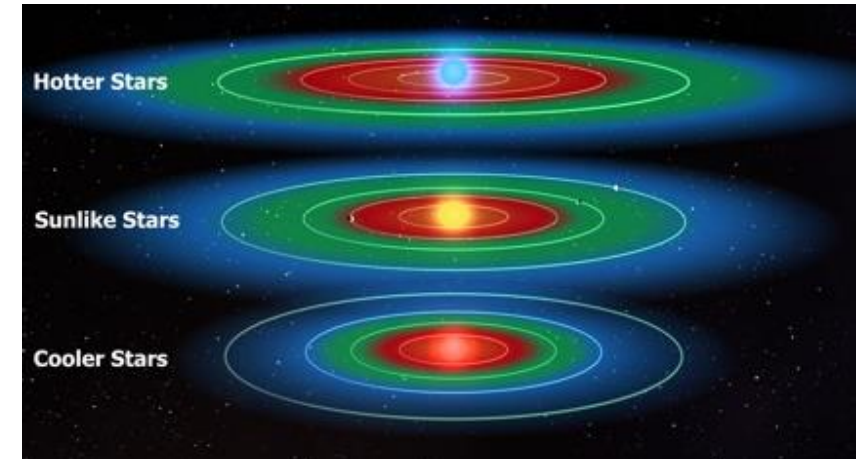
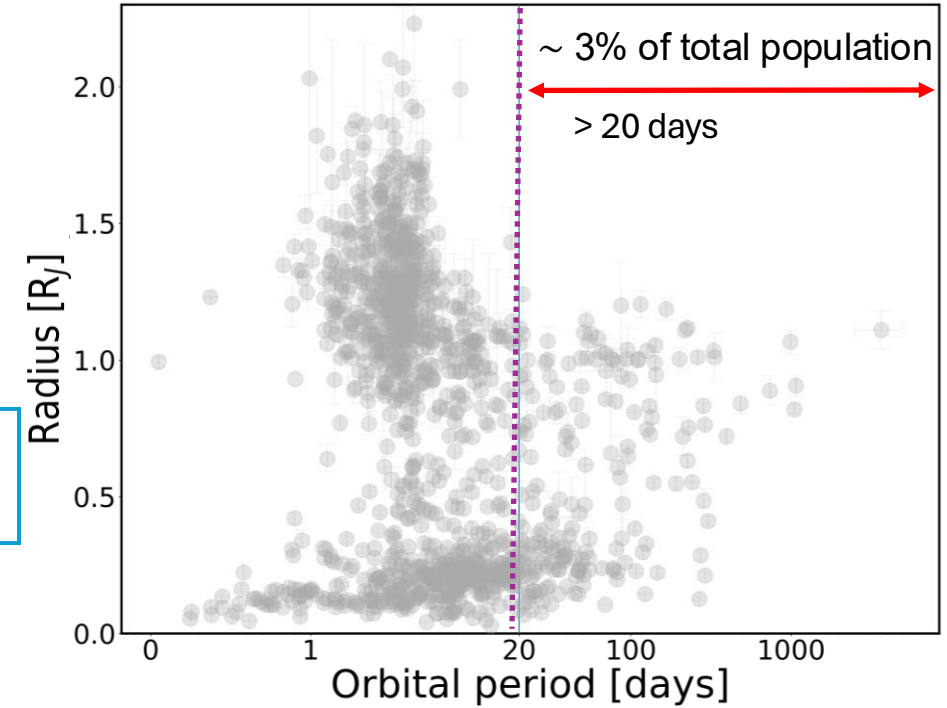


Top: known exoplanets from NASA archival data (June, 2025) with mass and radius accuracy of better than 30%. Bottom: Schematic of habitable zone of different planets (Credit: Lissauer+, 2018).

Why long-period planets are interesting?

- **Probe planets in the habitable zone**, as habitable zone around approximately M4/earlier spectral type stars is longer than ~ 11 days (Kopparapu+, 2013).

Low number of detected habitable zone planet \Leftrightarrow Low number of long-period planets detection



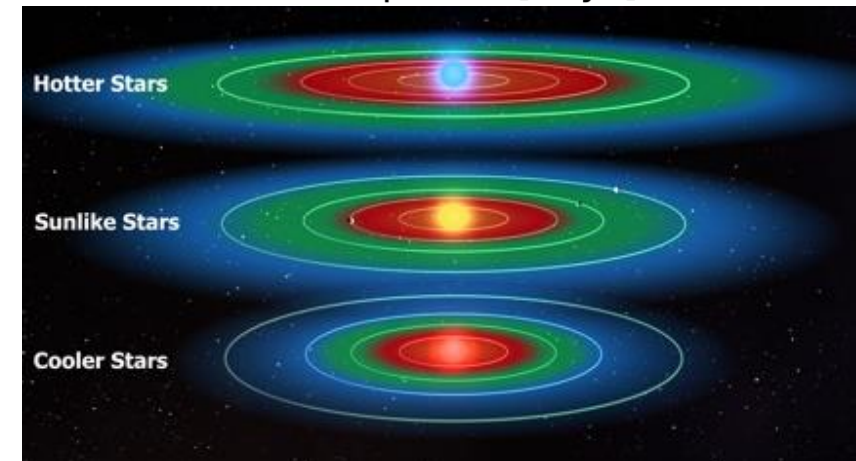
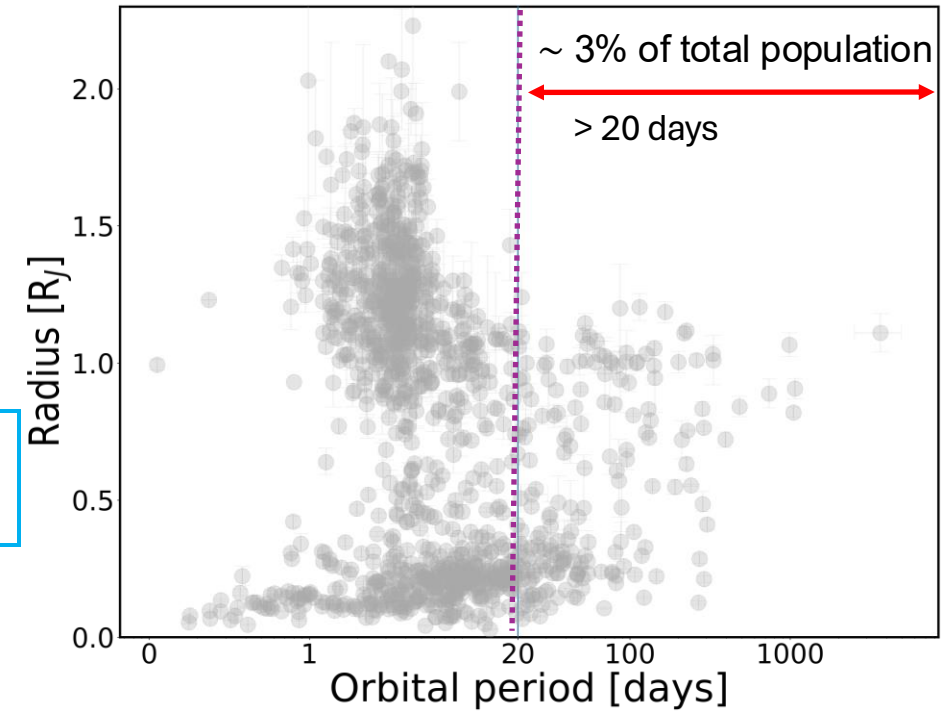
Top: known exoplanets from NASA archival data (June, 2025) with mass and radius accuracy of better than 30%. Bottom: Schematic of habitable zone of different planets (Credit: Lissauer+, 2018).

Why long-period planets are interesting?

- **Probe planets in the habitable zone**, as habitable zone around approximately M4/earlier spectral type stars is longer than ~ 11 days (Kopparapu+, 2013).

Low number of detected habitable zone planet \Leftrightarrow Low number of long-period planets detection

- **Less affected by stellar influence due to large separations**, reducing tidal and proximity effects (e.g., atmospheric evaporation), which helps preserve migration signatures.



Top: known exoplanets from NASA archival data (June, 2025) with mass and radius accuracy of better than 30%. Bottom: Schematic of habitable zone of different planets (Credit: Lissauer+, 2018).

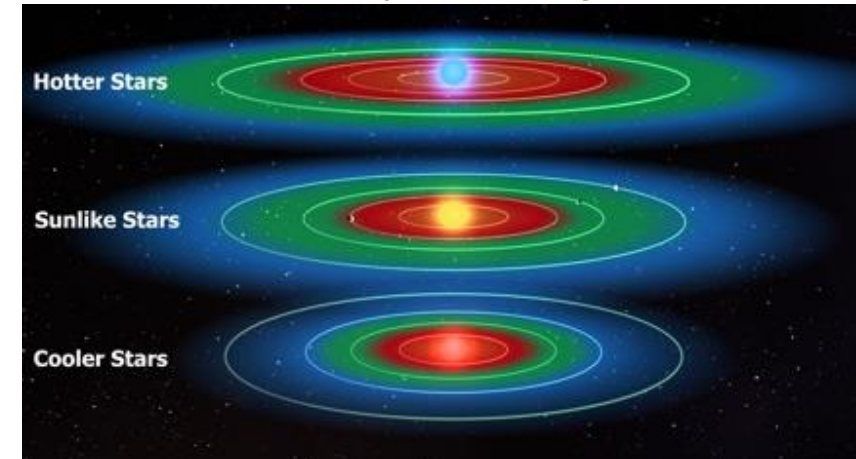
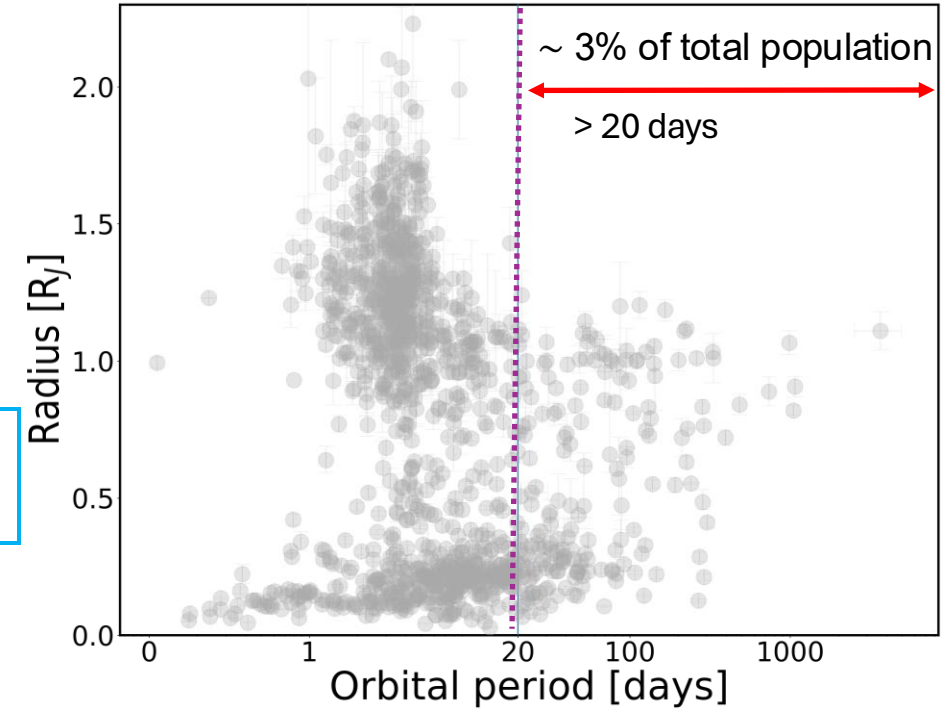
Why long-period planets are interesting?

- **Probe planets in the habitable zone**, as habitable zone around approximately M4/earlier spectral type stars is longer than ~ 11 days (Kopparapu+, 2013).

Low number of detected habitable zone planet \Leftrightarrow Low number of long-period planets detection

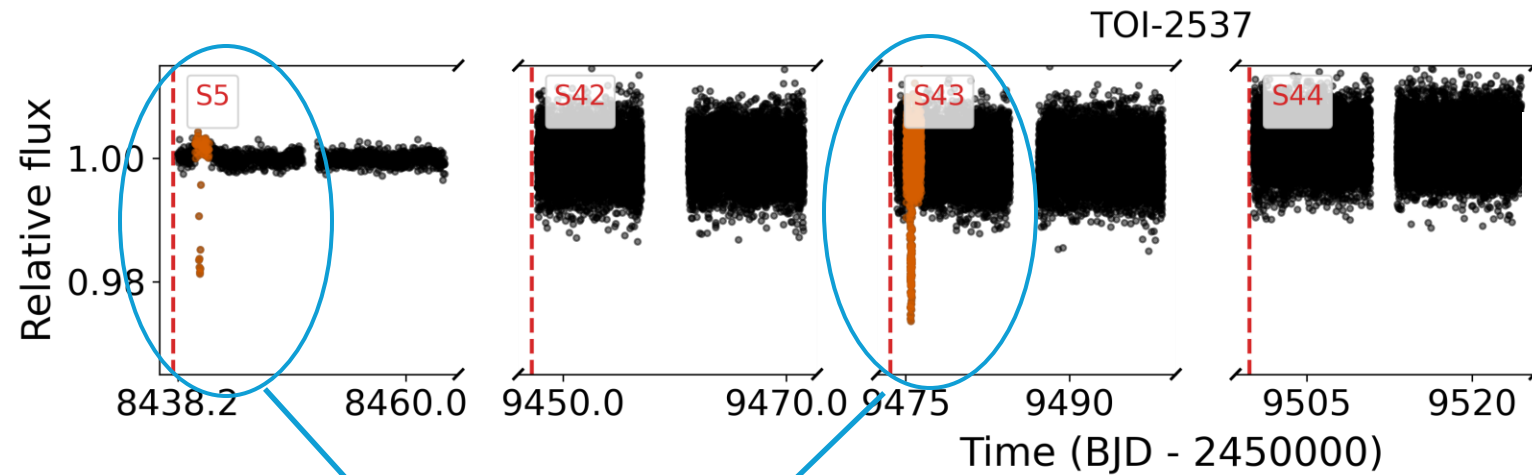
- **Less affected by stellar influence due to large separations**, reducing tidal and proximity effects (e.g., atmospheric evaporation), which helps preserve migration signatures.

Today I will present some of the results from our ongoing program to follow up TESS single-transit and duo candidates using SOPHIE.



Top: known exoplanets from NASA archival data (June, 2025) with mass and radius accuracy of better than 30%. Bottom: Schematic of habitable zone of different planets (Credit: Lissauer+, 2018).

TOI-2537 TESS photometry:

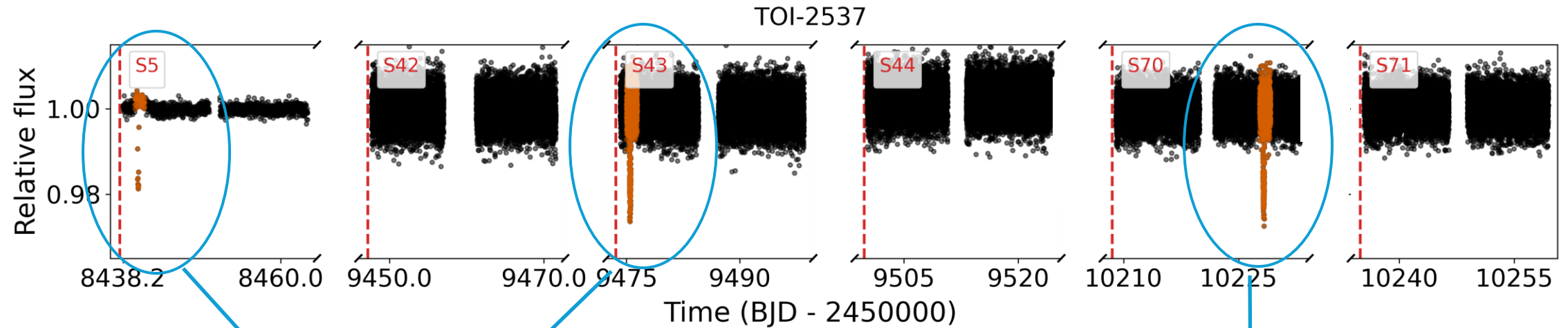


Initially only two transits were detected with separation of ~ 1000 d and no determined period.

Depth = 17910 ± 570 ppm

Duration = 4.9 h

TOI-2537 TESS photometry:



Initially only two transits were detected with separation of ~ 1000 d and no determined period.

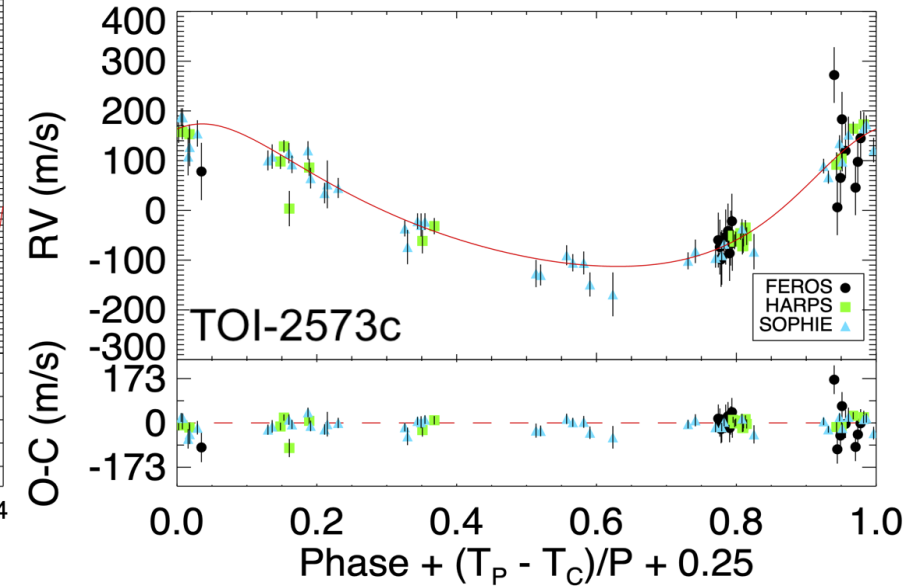
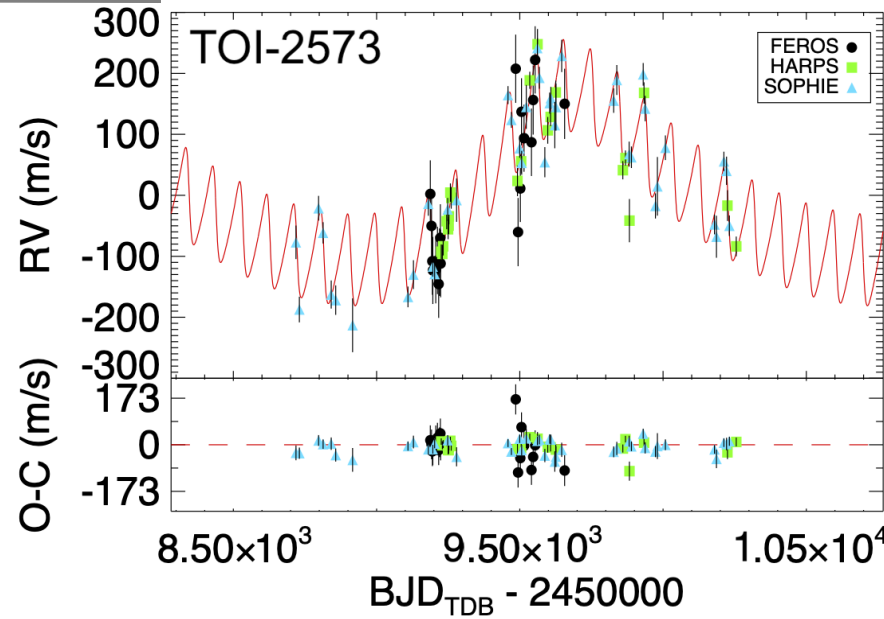
Later, a third transit of the TOI-2537b was detected.

Depth = 17910 ± 570 ppm

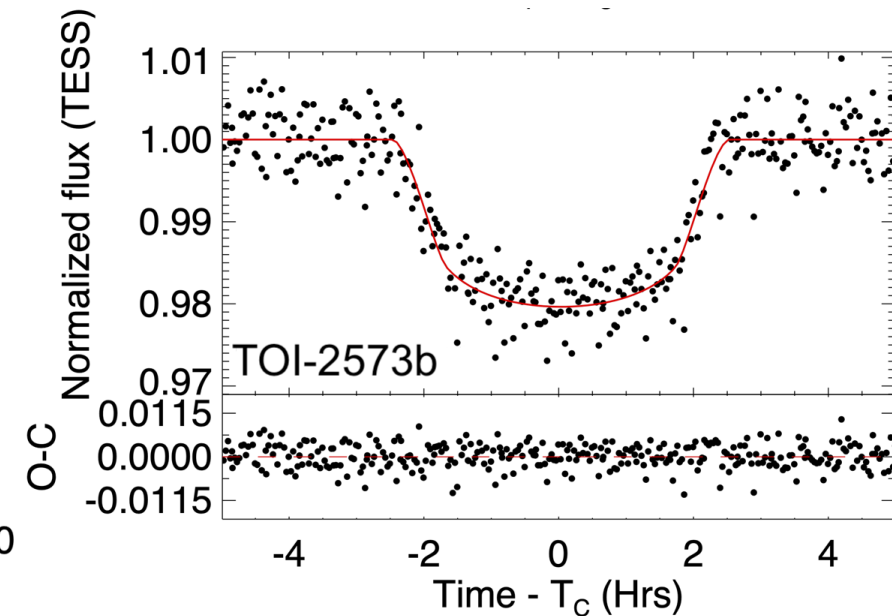
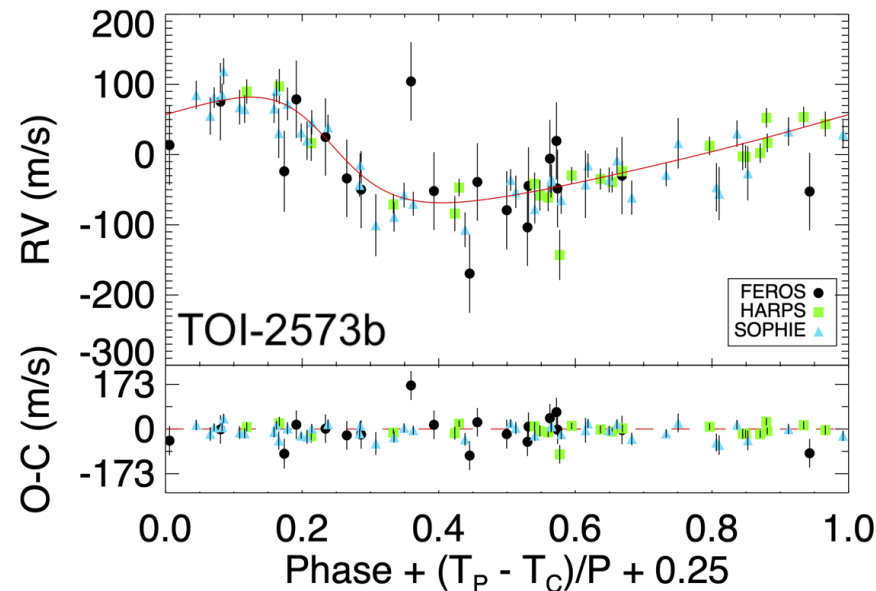
Duration = 4.9 h

TOI-2537 b & c :

(Heidari, Hebrard, et al 2024)

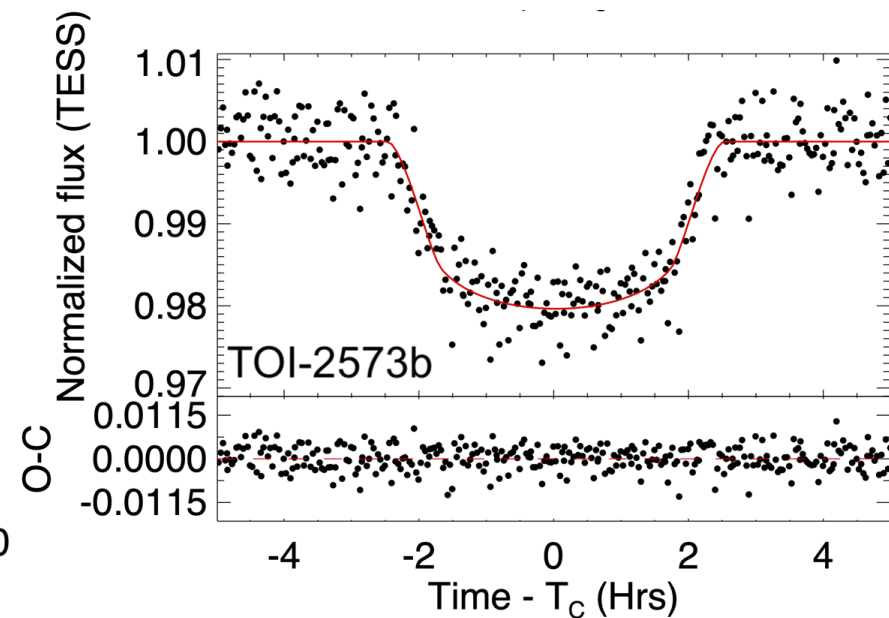
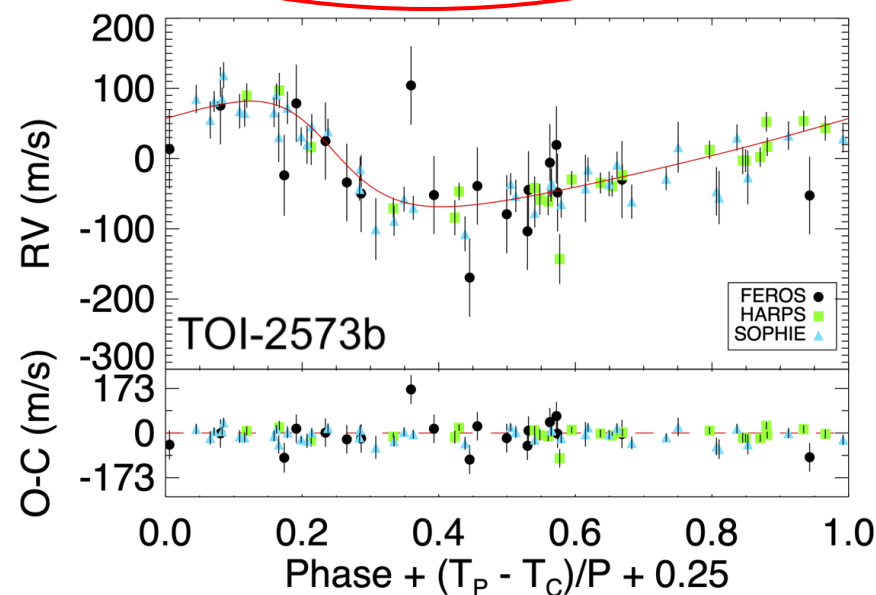
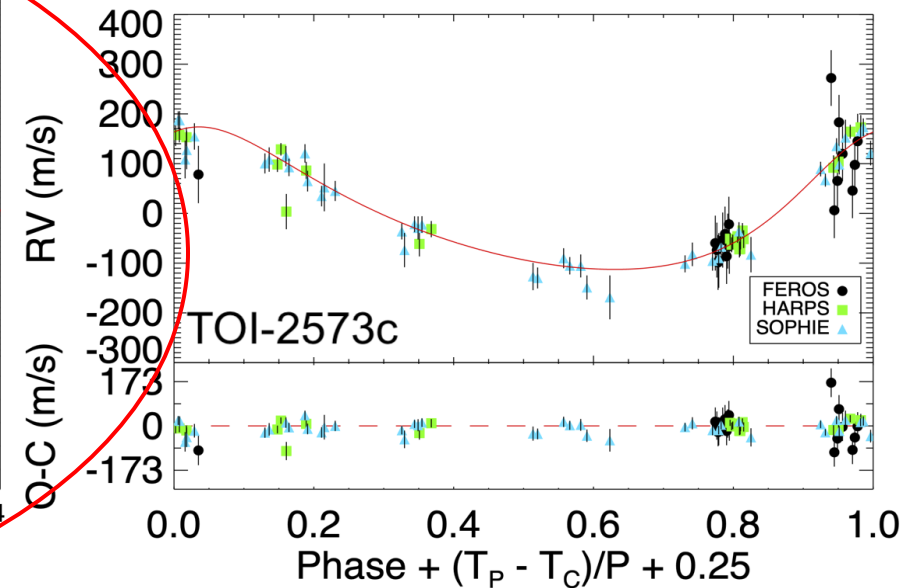
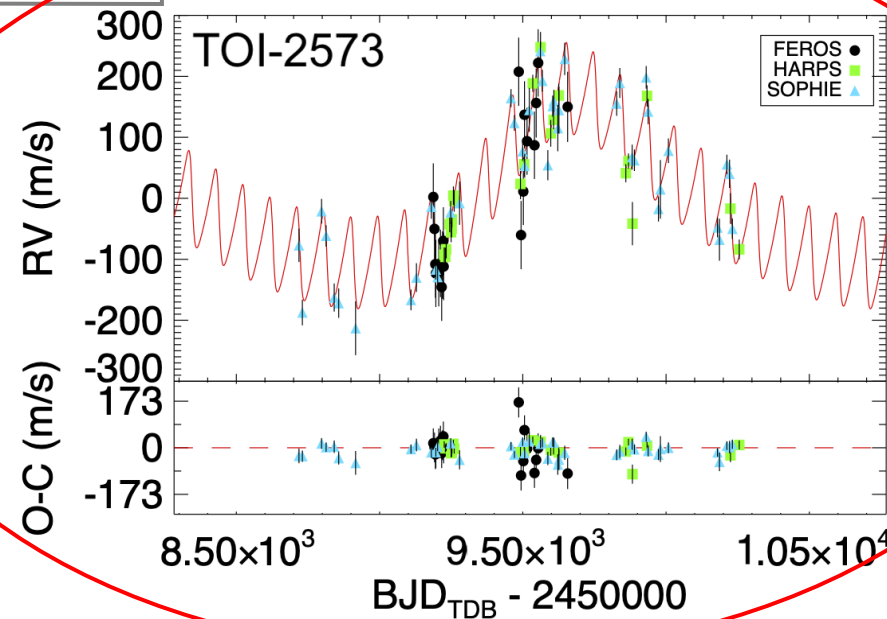


RV measurements of TOI-2537 (top-left), phase-folded RVs for TOI-2537c (top-right), phase-folded RVs (bottom-left) and light curves for TOI-2537b (bottom-right). The red lines represent the median models, accounting for TTVs as determined by EXOFASTv2. Residuals are displayed at the bottom of each panel.



TOI-2537 b & c :

(Heidari, Hebrard, et al 2024)

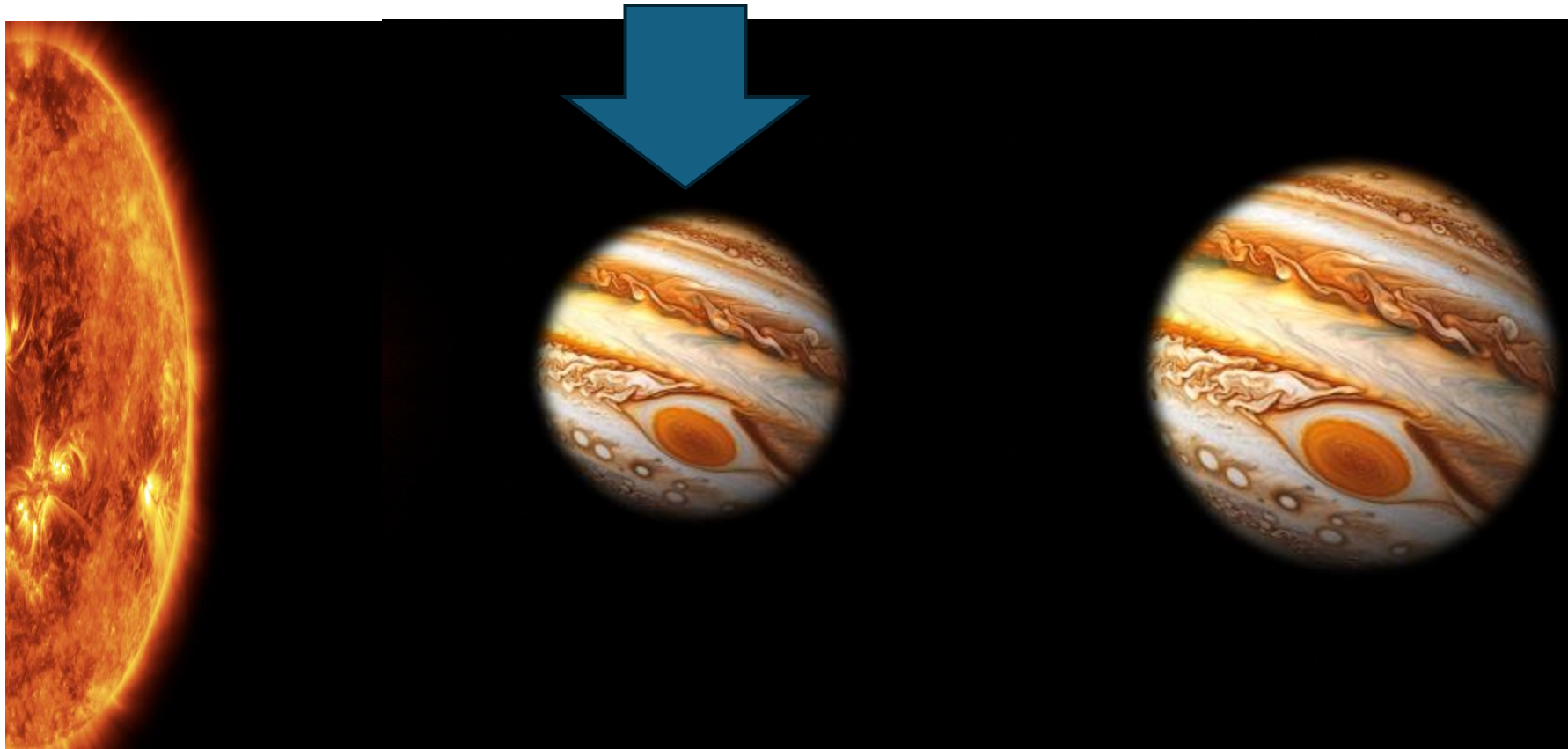


RV measurements of TOI-2537 (top-left), phase-folded RVs for TOI-2537c (top-right), phase-folded RVs (bottom-left) and light curves for TOI-2537b (bottom-right). The red lines represent the median models, accounting for TTVs as determined by EXOFASTv2. Residuals are displayed at the bottom of each panel.

TOI-2537 b & c :

(Heidari, Hebrard, et al 2024)

P_planet b (d)	94.1 ± 0.2
R_planet b (R_J)	1.00 ± 0.03
M_planet b (M_J)	1.31 ± 0.09
e	0.36 ± 0.04

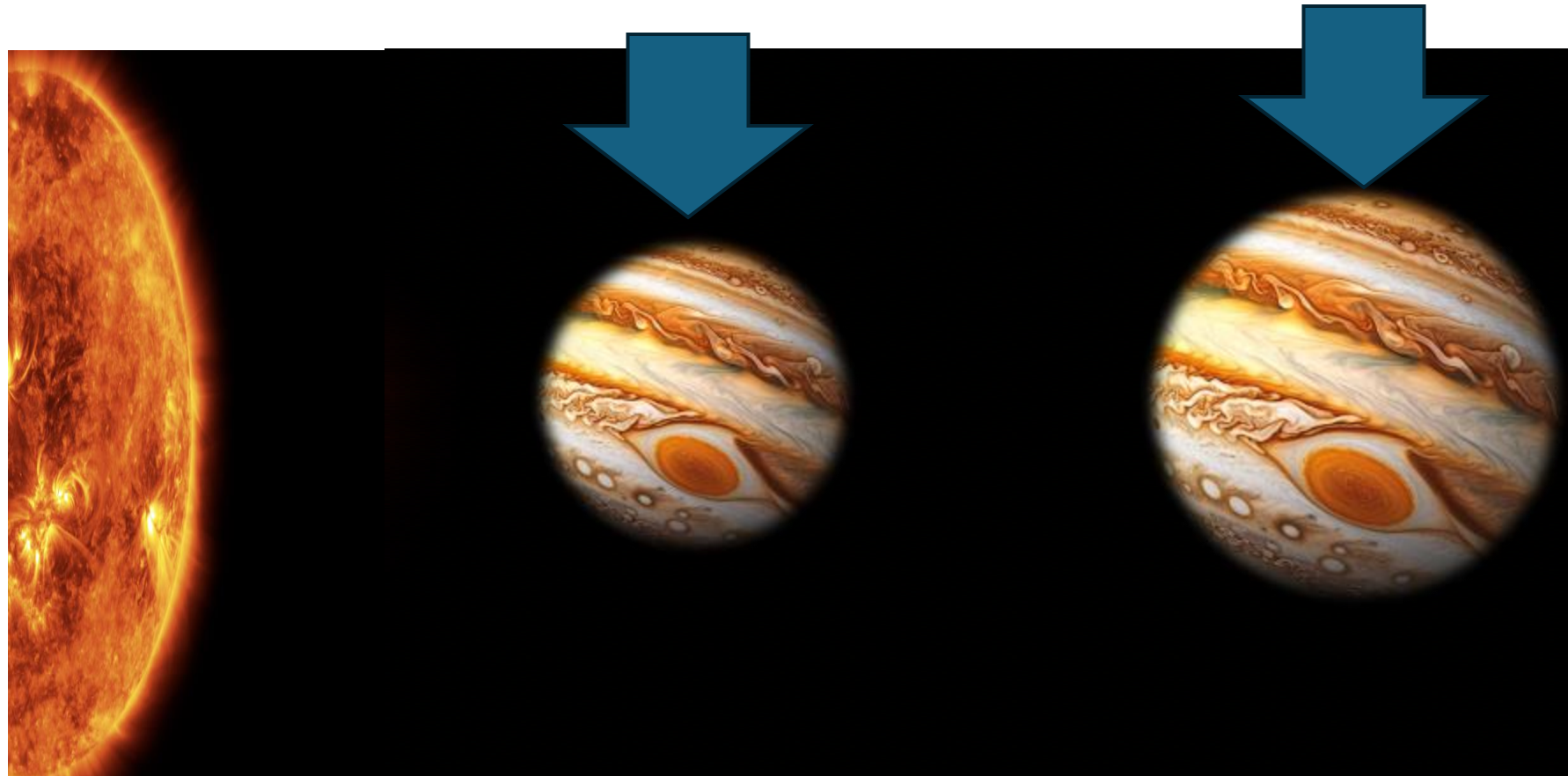


TOI-2537 b & c :

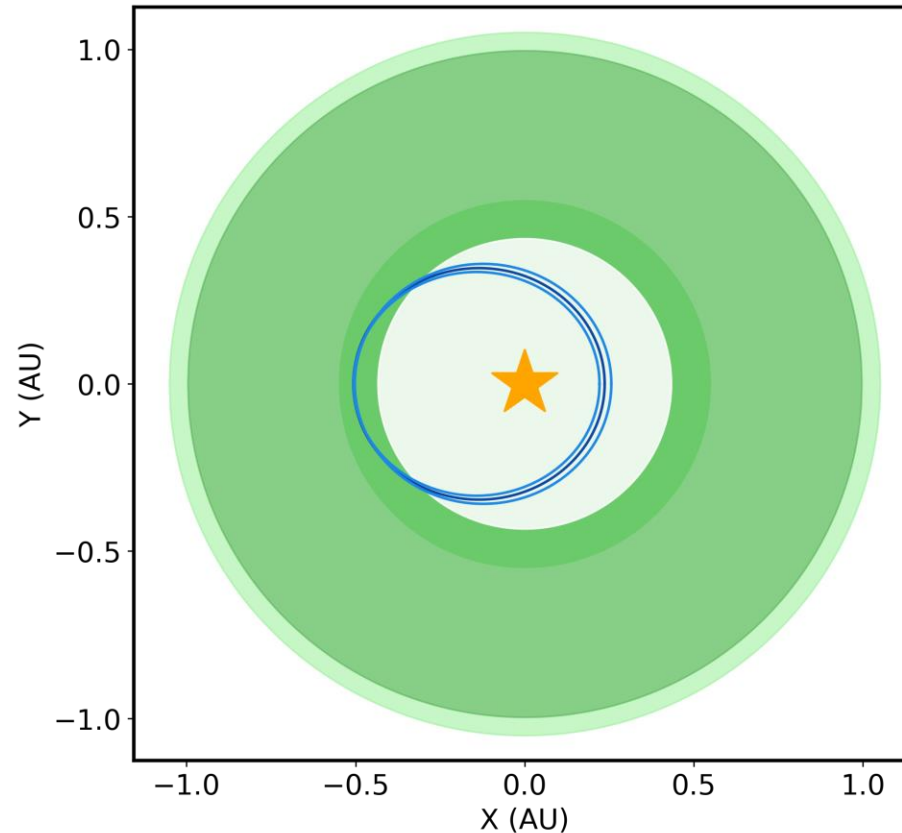
(Heidari, Hebrard, et al 2024)

P_planet b (d)	94.1 ± 0.2
R_planet b (R _J)	1.00 ± 0.03
M_planet b (M _J)	1.31 ± 0.09
e	0.36 ± 0.04

P_planet c (d)	1920 ± 185
M_sini_planet c (M _J)	8.10 ± 0.80
e	0.29 ± 0.06



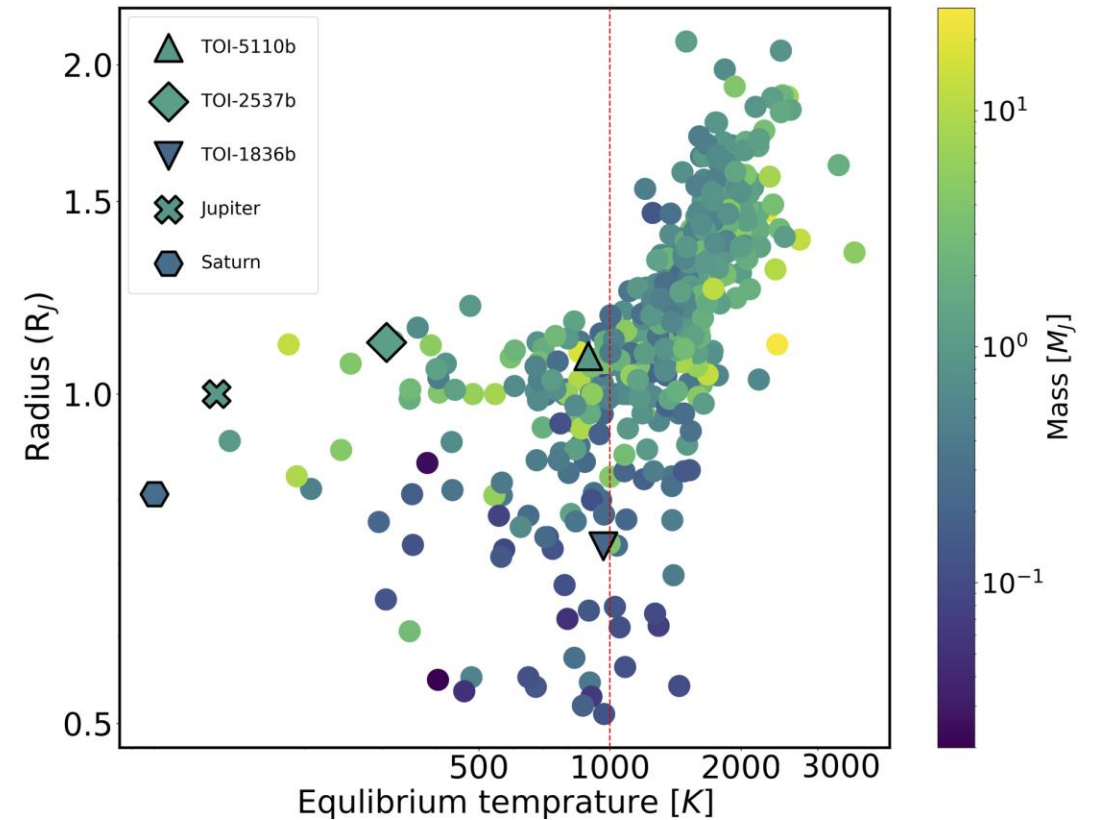
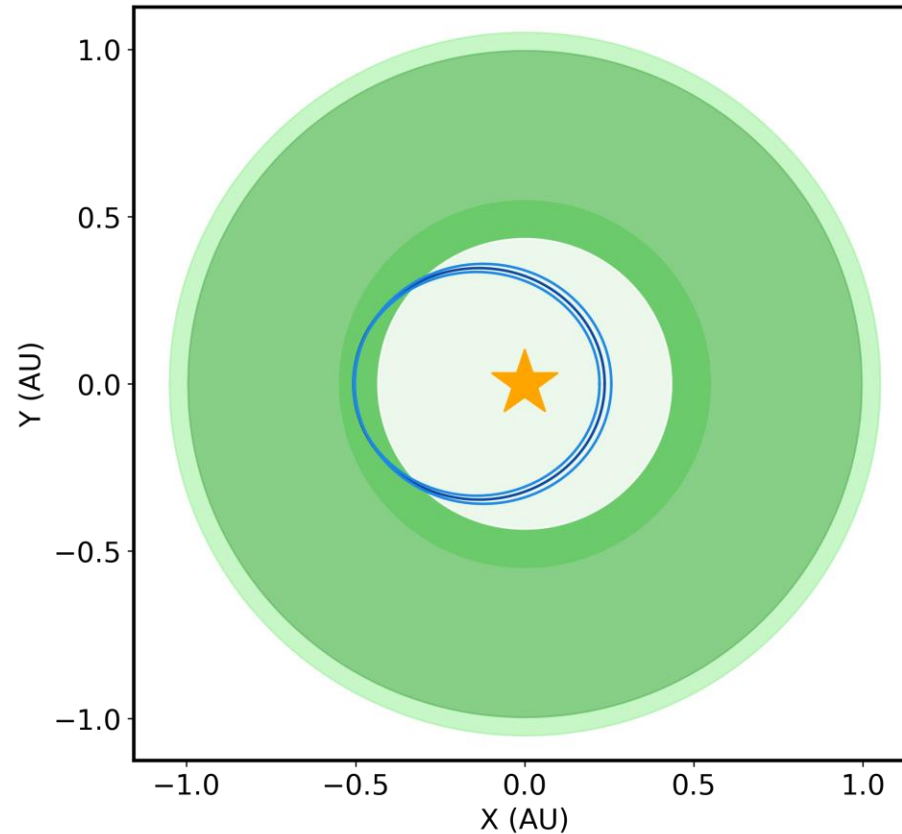
TOI-2537 b :

[\(Heidari, Hebrard, et al 2024\)](#)Teff= 307 ± 15 K

Left: The configuration of the TOI-2537b within the habitable zone. The orbit of TOI-2537b is depicted in dark blue, with its uncertainties represented by light blue. The habitable zone boundaries are indicated by green-shaded regions, representing the empirical habitable zone boundaries for recent Venus (inner boundary), runaway greenhouse (middle boundaries), and early Mars (outer boundary). These boundaries are computed following the results from Kopparapu et al. (2014).

TOI-2537 b :

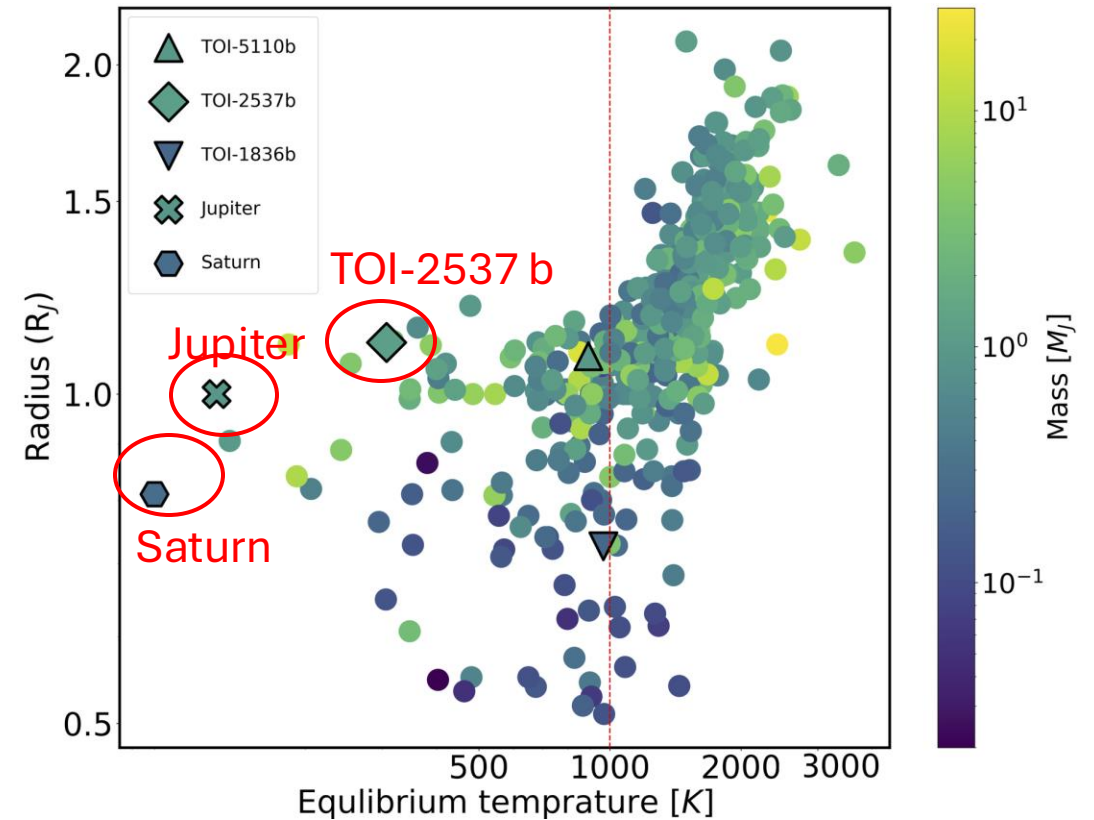
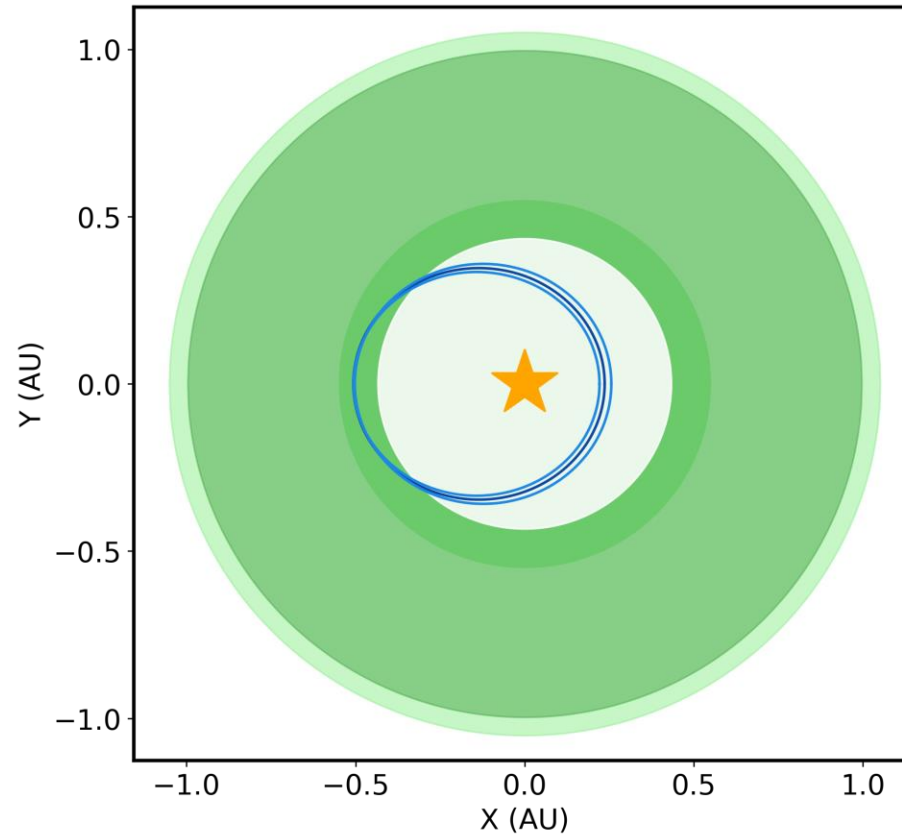
(Heidari, Hebrard, et al 2024)

Teff = 307 ± 15 K

Left: The configuration of the TOI-2537b within the habitable zone. The orbit of TOI-2537b is depicted in dark blue, with its uncertainties represented by light blue. The habitable zone boundaries are indicated by green-shaded regions, representing the empirical habitable zone boundaries for recent Venus (inner boundary), runaway greenhouse (middle boundaries), and early Mars (outer boundary). These boundaries are computed following the results from Kopparapu et al. (2014). *Right:* The radius-equilibrium temperature of known giant ($R > 0.5 R_J$) transiting planets with accurate mass and radii (Otegi et al. 2020). The red vertical line indicates the empirical inflation boundary (Fortney et al. 2021), where planet radii are seen to increase with equilibrium temperature.

TOI-2537 b :

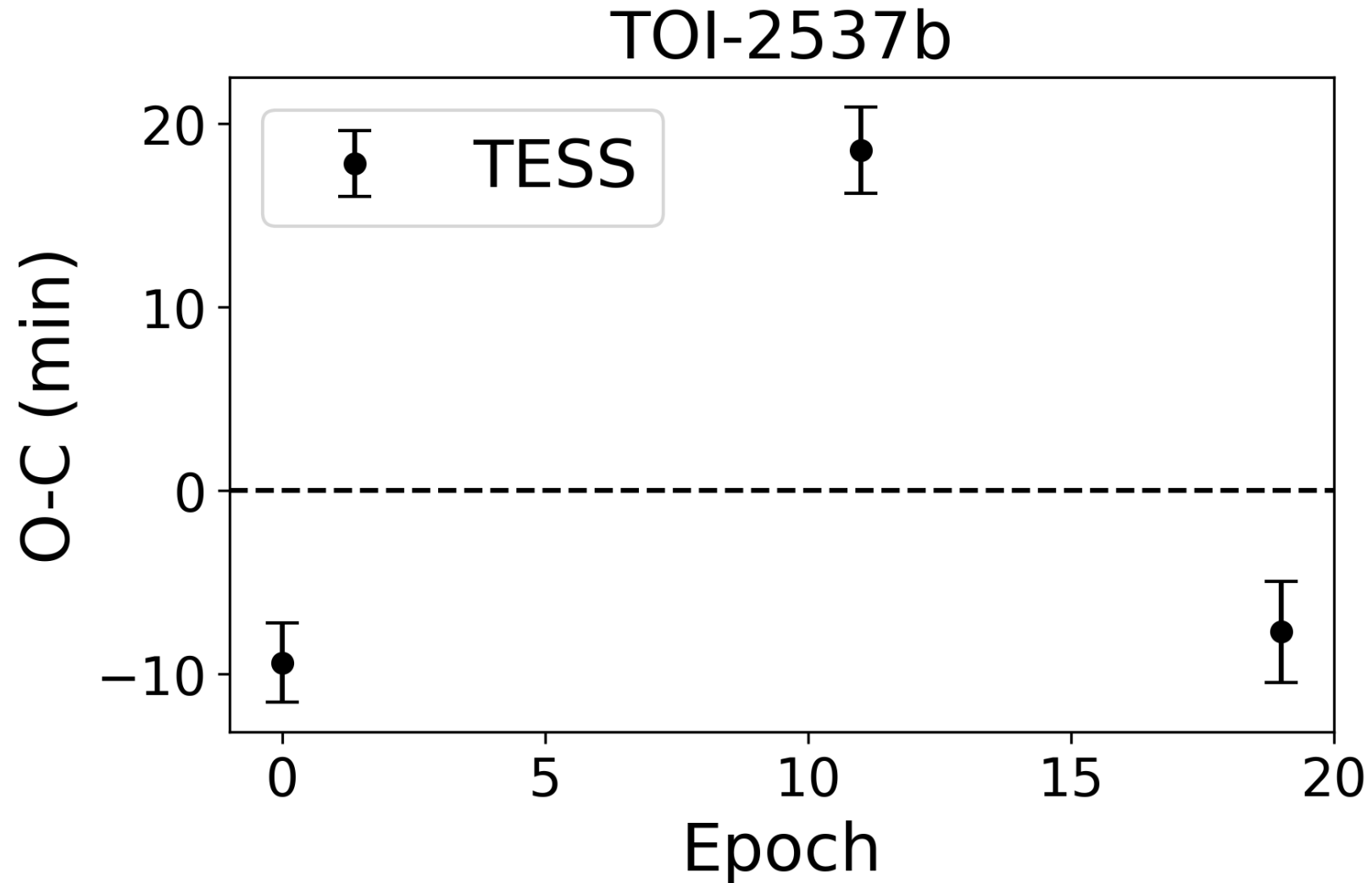
(Heidari, Hebrard, et al 2024)

Teff = 307 ± 15 K

Left: The configuration of the TOI-2537b within the habitable zone. The orbit of TOI-2537b is depicted in dark blue, with its uncertainties represented by light blue. The habitable zone boundaries are indicated by green-shaded regions, representing the empirical habitable zone boundaries for recent Venus (inner boundary), runaway greenhouse (middle boundaries), and early Mars (outer boundary). These boundaries are computed following the results from Kopparapu et al. (2014). *Right:* The radius-equilibrium temperature of known giant ($R > 0.5 R_J$) transiting planets with accurate mass and radii (Otegi et al. 2020). The red vertical line indicates the empirical inflation boundary (Fortney et al. 2021), where planet radii are seen to increase with equilibrium temperature.

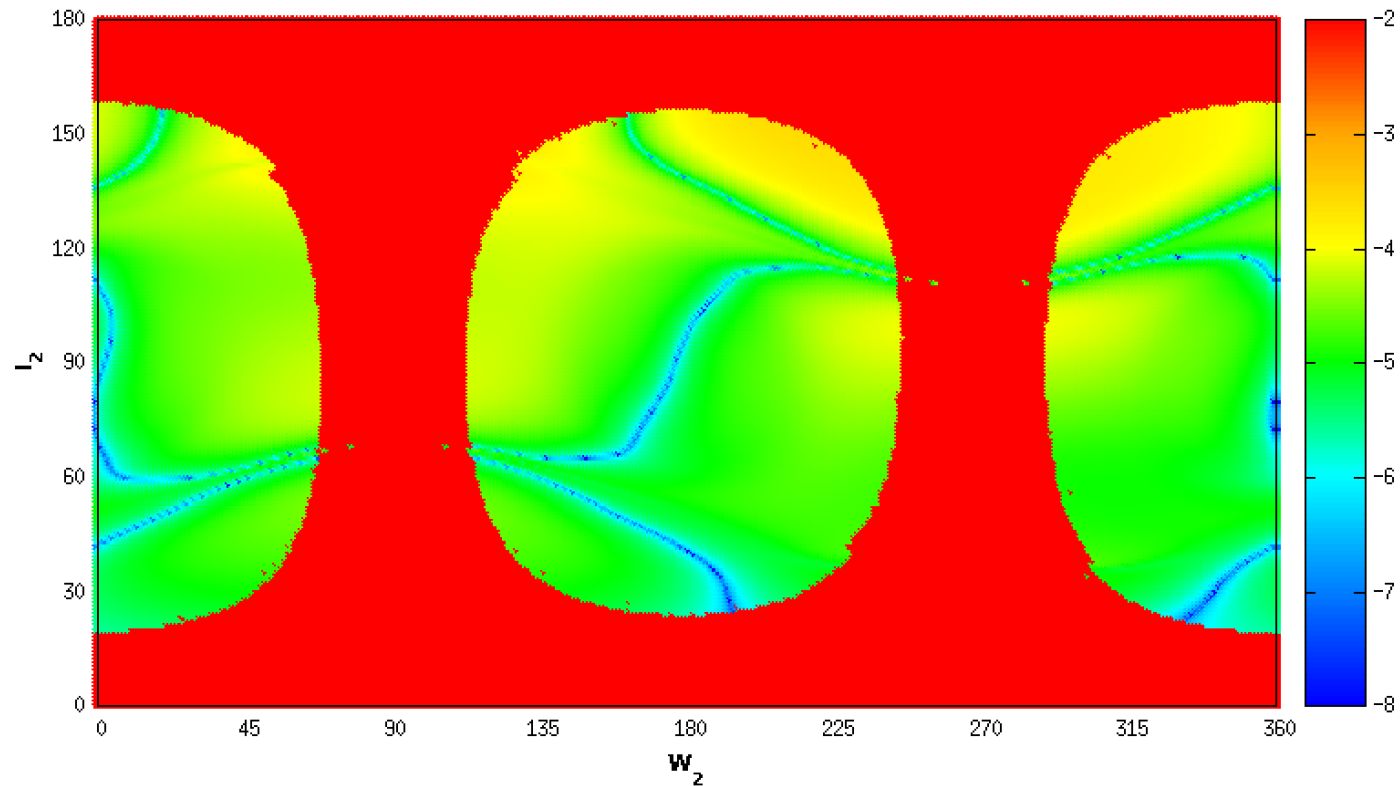
TTVs of TOI-2537 b:
(Heidari, Hebrard, et al 2024)

TTV peak to peak
variations: ~ 28 min



The difference between the predicted and observed midtransit times for TOI-2537b.

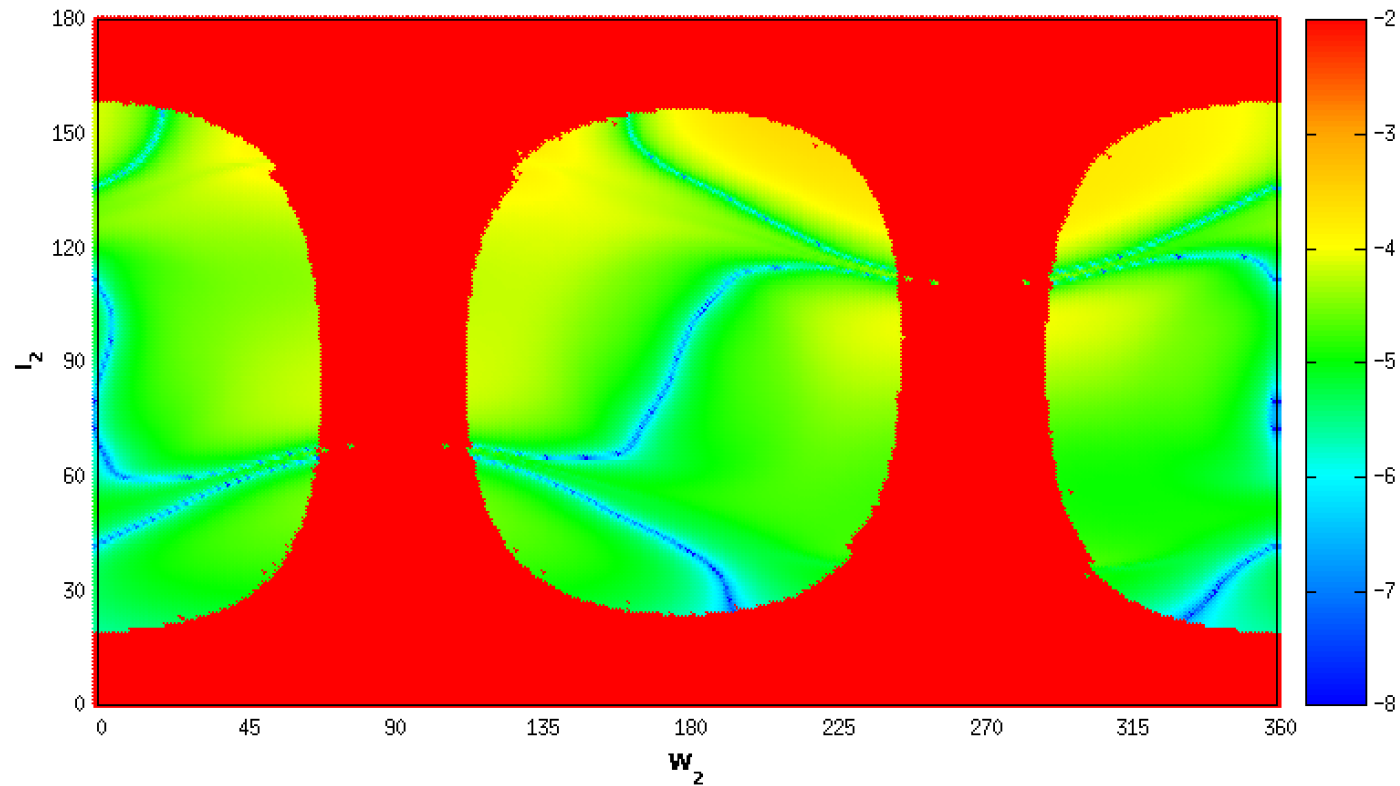
Preliminary dynamical analyses of the TOI-2537 system :
(Heidari, Hebrard, et al 2024)



Left: Stability analysis of the TOI-2537 planetary system. For fixed initial conditions, the phase space of the system is explored by varying the two unknown parameters of TOI-2537c's orbit, namely the longitude of its ascending node and its inclination. The red zone corresponds to highly unstable orbits, while the green-blue regions can be assumed to be stable on a billion-year timescale.

Preliminary dynamical analyses of the TOI-2537 system :
(Heidari, Hebrard, et al 2024)

Mass of planet $c < 20 \text{ MJ}$

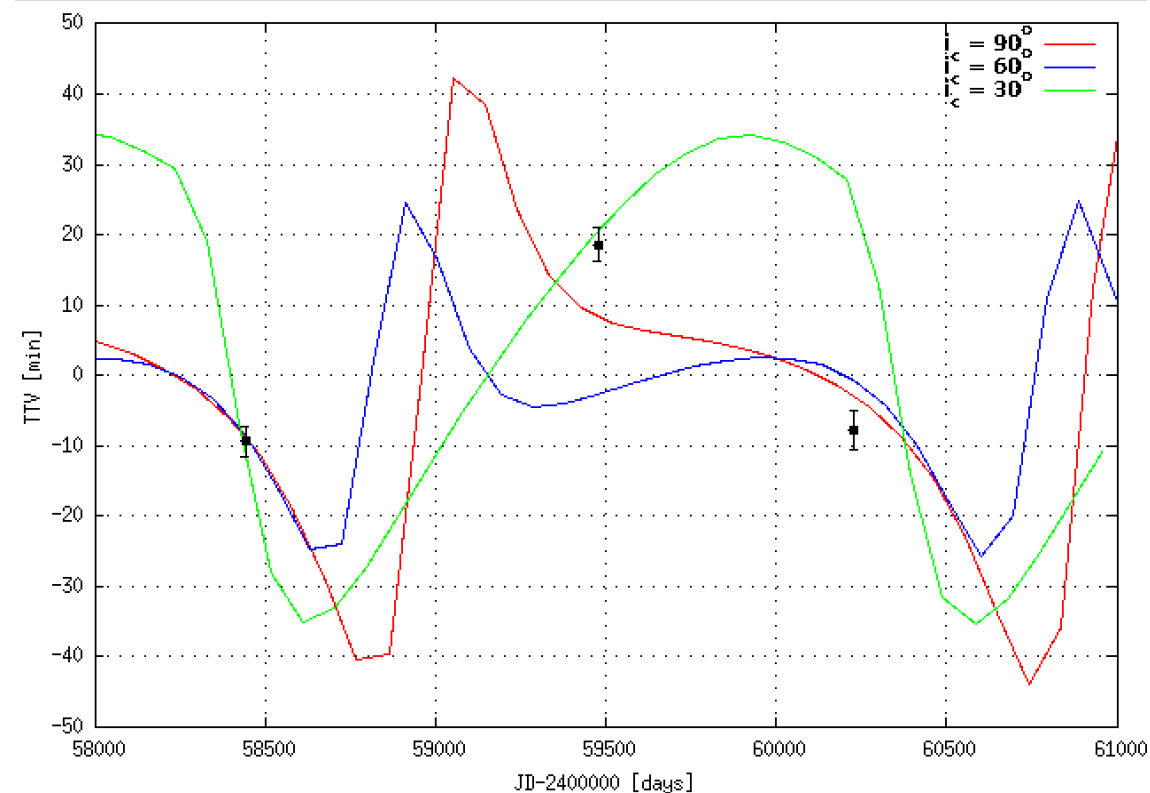
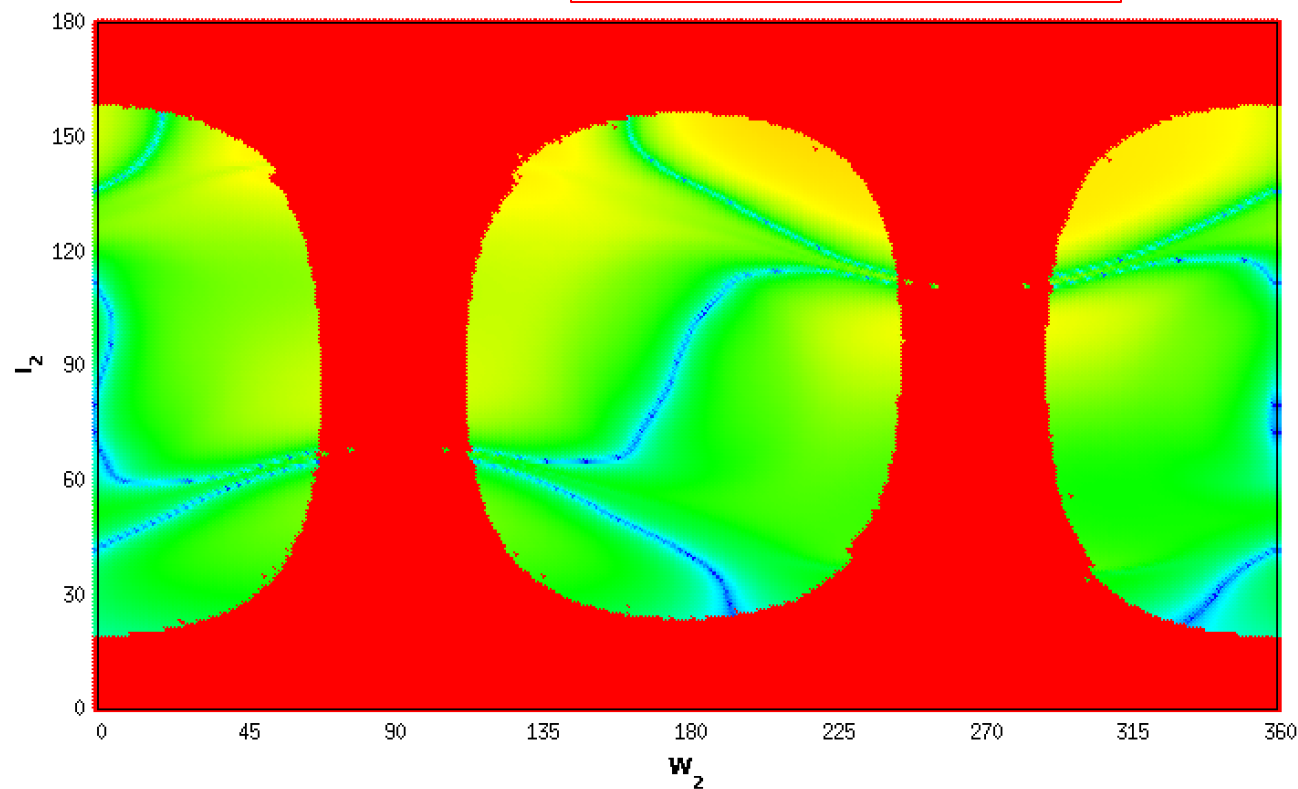


Left: Stability analysis of the TOI-2537 planetary system. For fixed initial conditions, the phase space of the system is explored by varying the two unknown parameters of TOI-2537c's orbit, namely the longitude of its ascending node and its inclination. The red zone corresponds to highly unstable orbits, while the green-blue regions can be assumed to be stable on a billion-year timescale.

Preliminary dynamical analyses of the TOI-2537 system :

(Heidari, Hebrard, et al 2024)

Mass of planet c < 20 MJ

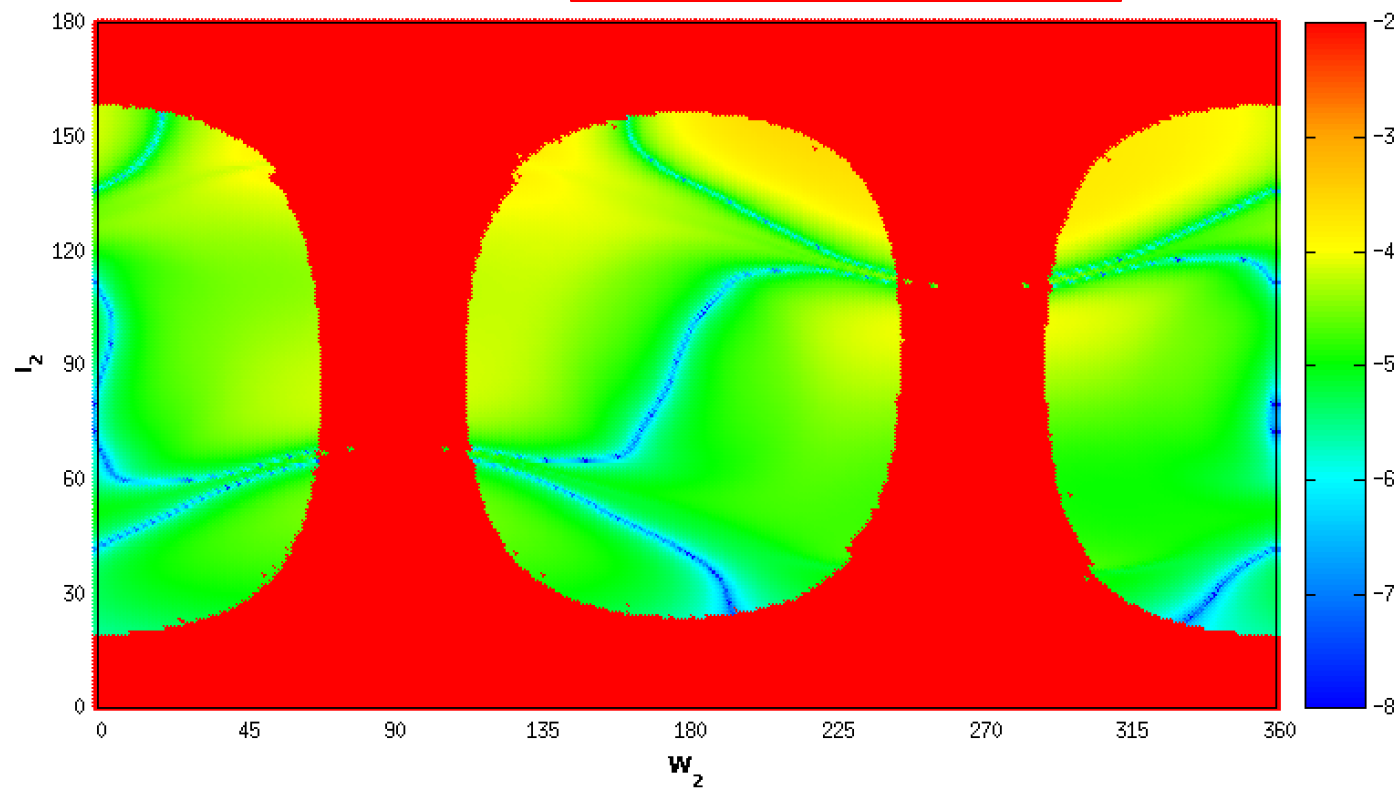


Left: Stability analysis of the TOI-2537 planetary system. For fixed initial conditions, the phase space of the system is explored by varying the two unknown parameters of TOI-2537c's orbit, namely the longitude of its ascending node and its inclination. The red zone corresponds to highly unstable orbits, while the green-blue regions can be assumed to be stable on a billion-year timescale. Right: Transit-timing variations for the TOI-2537b planet. The simulated TTVs have similar orders of magnitude to the measured TTVs.

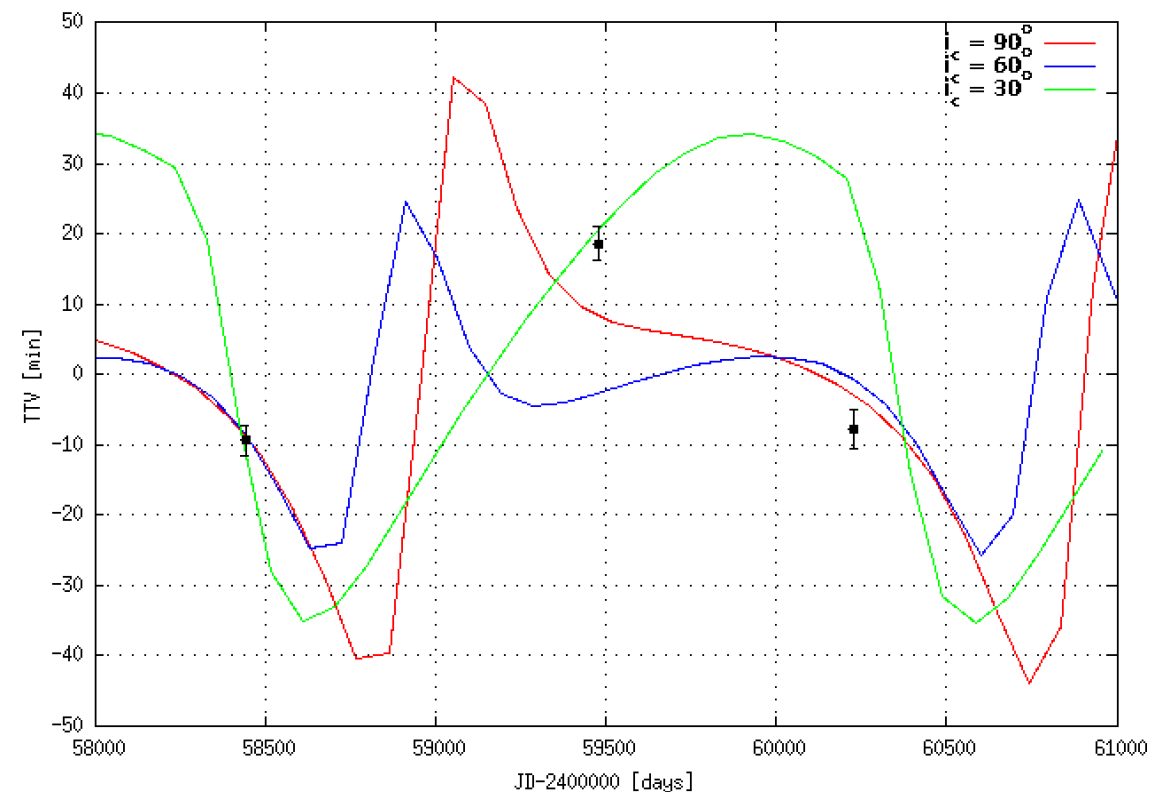
Preliminary dynamical analyses of the TOI-2537 system :

(Heidari, Hebrard, et al 2024)

Mass of planet c < 20 MJ



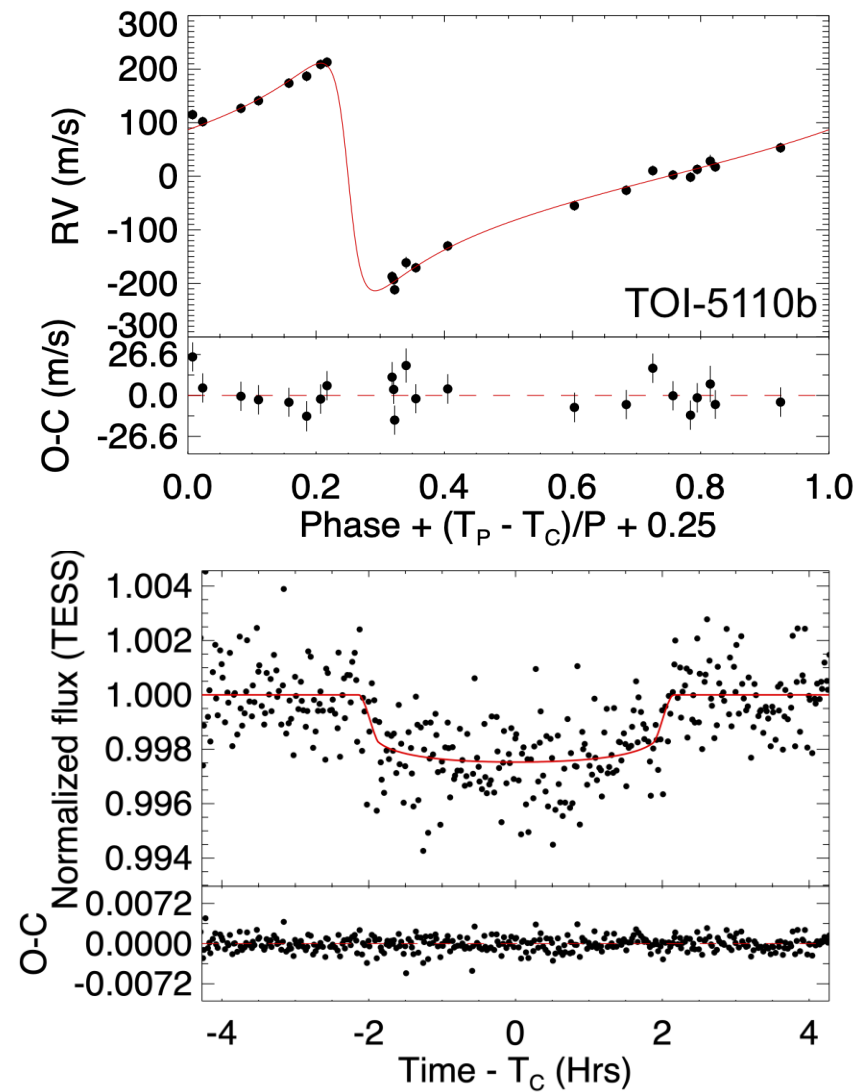
The TTVs observed in TOI-2537b are likely to be caused by TOI-2537c. New transit observations are required.



Left: Stability analysis of the TOI-2537 planetary system. For fixed initial conditions, the phase space of the system is explored by varying the two unknown parameters of TOI-2537c's orbit, namely the longitude of its ascending node and its inclination. The red zone corresponds to highly unstable orbits, while the green-blue regions can be assumed to be stable on a billion-year timescale. Right: Transit-timing variations for the TOI-2537b planet. The simulated TTVs have similar orders of magnitude to the measured TTVs.

TOI-5110 b (Heidari, Hebrard, et al 2024):

P (d)	30.1588+/-0.0001
R (R _J)	1.07 +/- 0.05
M (M _J)	2.90 ± 0.13
Teq (K)	976+/- 32 (1900-740)
e	0.75+/- 0.030



RVs (top) and TESS photometric data (bottom) phase-folded to the orbital period of the planet candidate.

TOI-5110 b (Heidari, Hebrard, et al 2024):

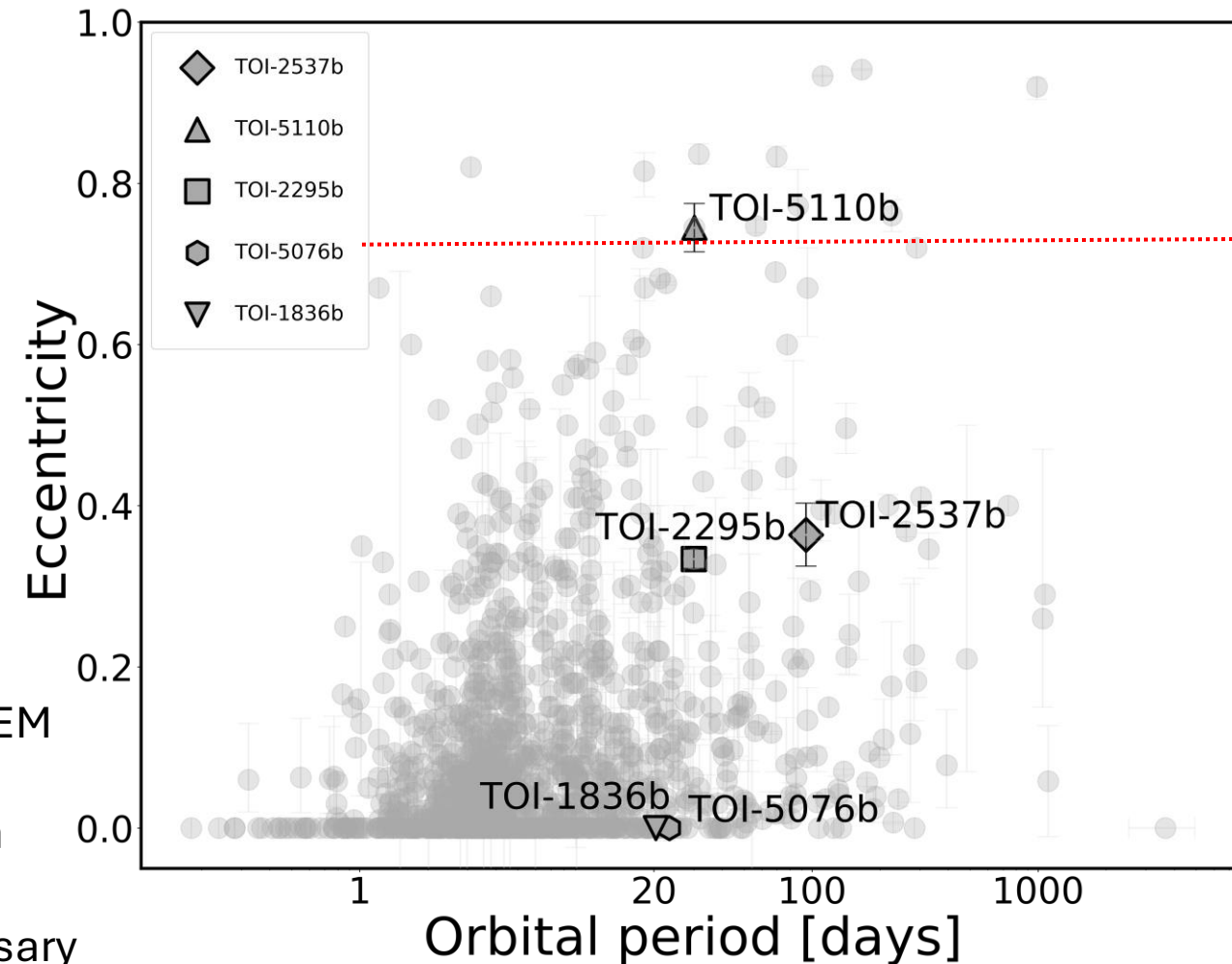
Orbital eccentricity is one of the key features in the study of exoplanet formation and evolution (Ribas & Miralda-Escudé 2007; Takeda & Rasio 2005).

Possible origins:

Angular momentum exchange with a perturber leading to HEM

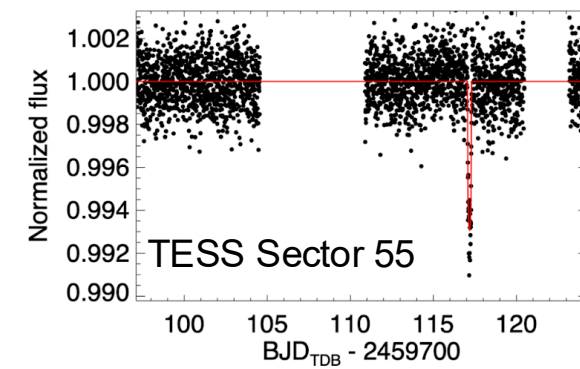
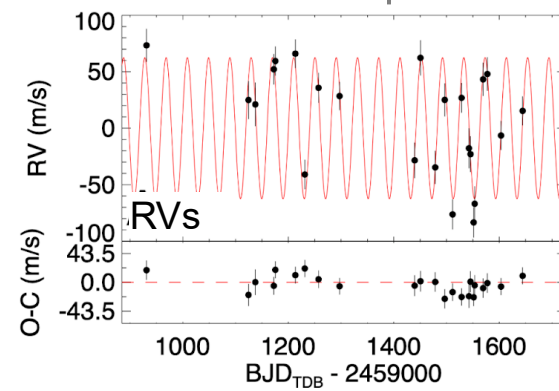
i.e., a short-period, low-mass companion hidden in the data

Additional RV observations with higher precision are necessary



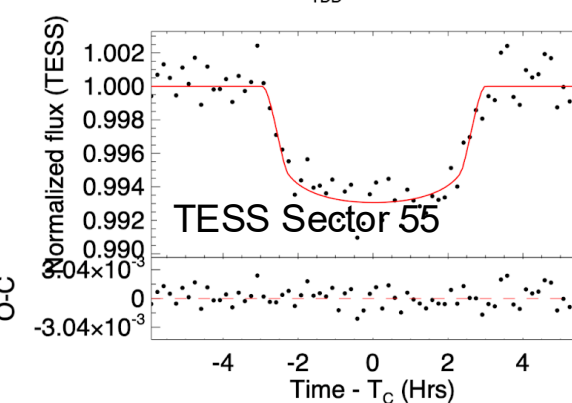
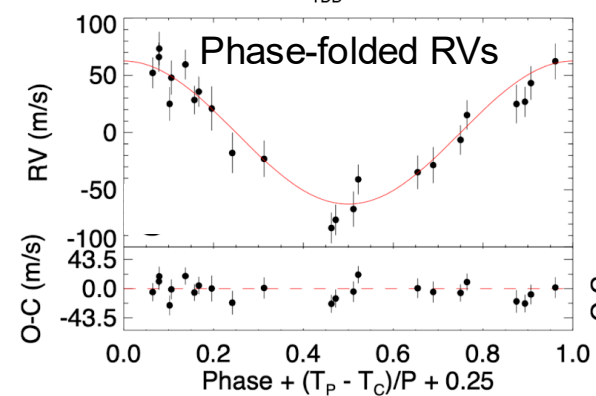
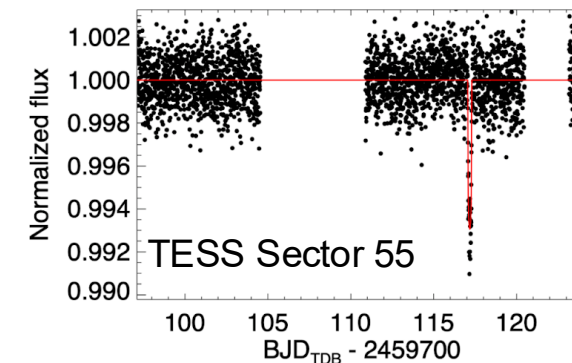
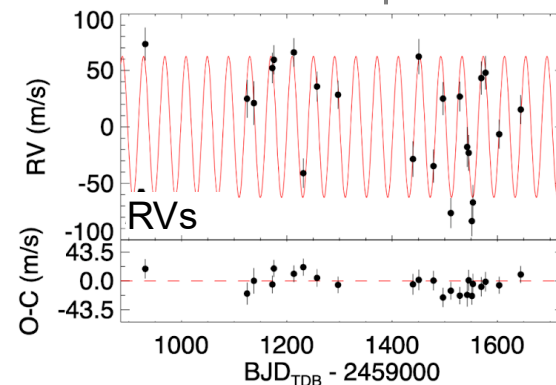
Eccentricity-period panel highlights the unique position of TOI-5110b as one of the most eccentric planets known to date.

TOI-X (Heidari, Hebrard, et al in prep):



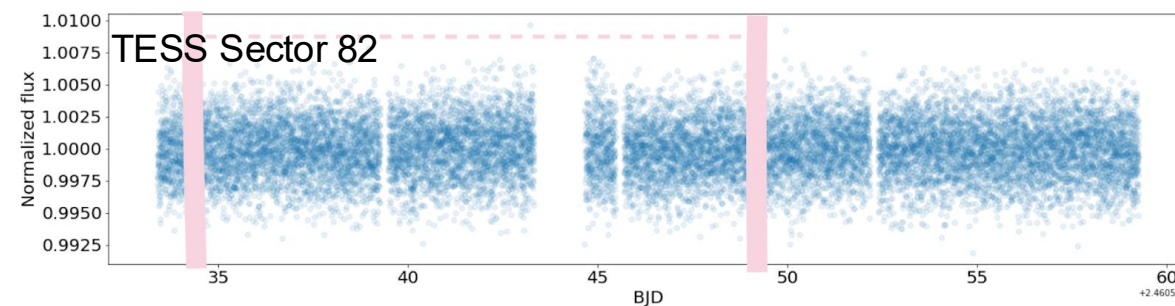
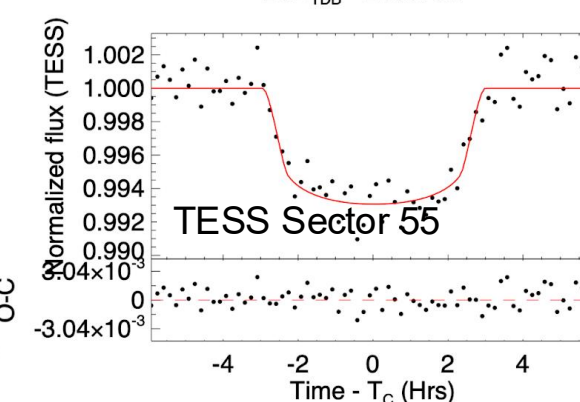
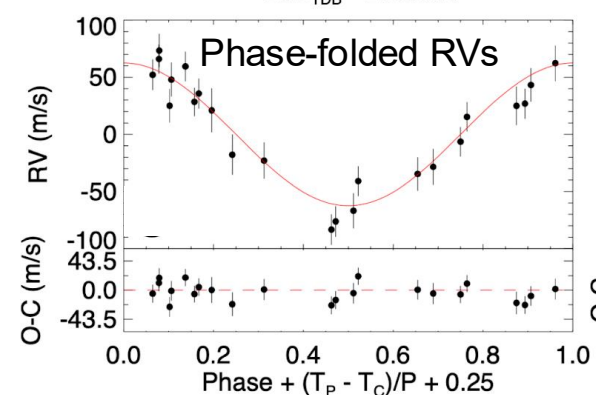
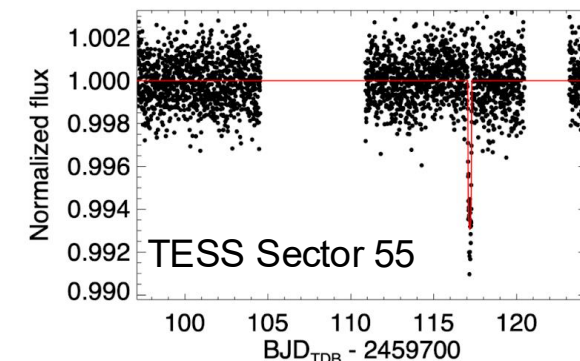
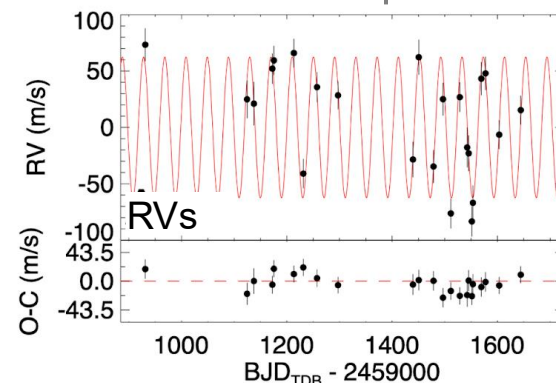
TOI-X (Heidari, Hebrard, et al in prep):

P (d)	40.36 ± 0.01
R (RJ)	0.91 ± 0.05
Mass (MJ)	1.07 ± 0.10



TOI-X (Heidari, Hebrard, et al in prep):

P (d)	40.36 ± 0.01
R (RJ)	0.91 ± 0.05
Mass (MJ)	1.07 ± 0.10



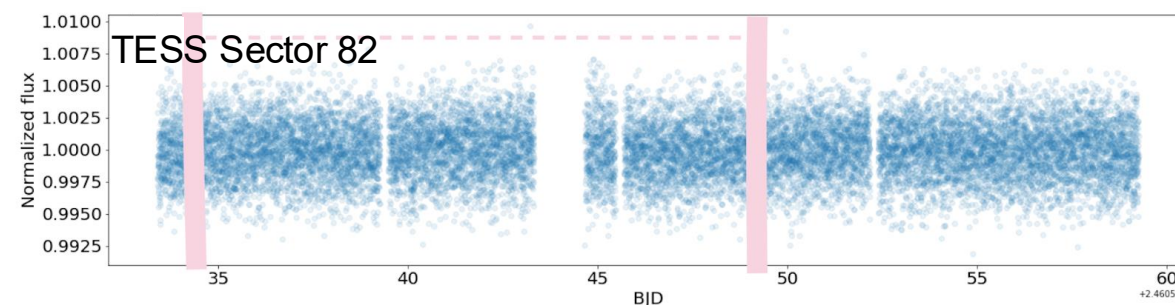
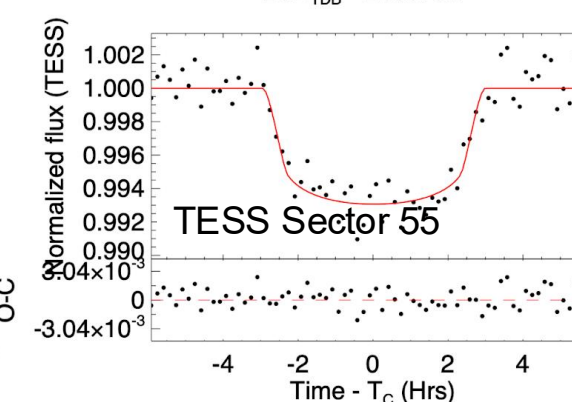
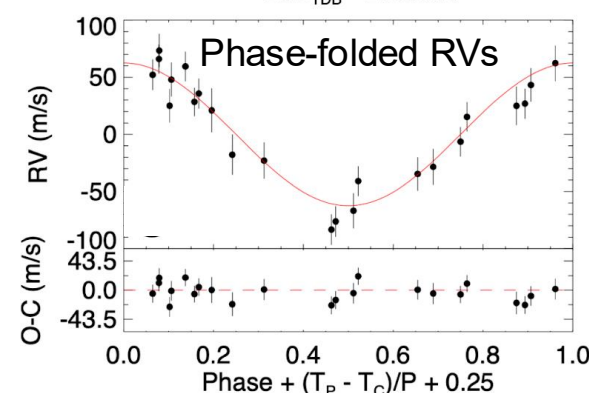
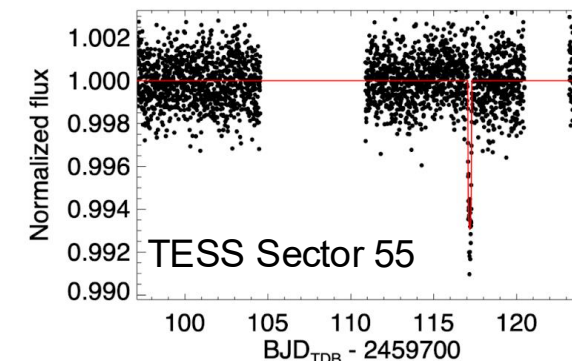
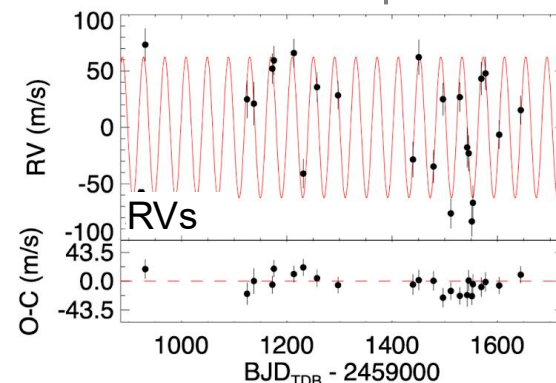
Top-left: SOPHIE RV time series. *Top-right:* TESS Sector 55 light curve. *Middle-left:* Phase-folded RV measurements. *Middle-right:* Phase-folded TESS sector 55 transit light curve. In all panels, the red curves show the best-fit median models obtained using *EXOFASTv2*, with residuals displayed beneath each plot. *Bottom* shows the TESS Sector 82 light curve, where the horizontal pink line indicates the predicted transit time based on the joint analysis of RV and photometric data of sector 55.

TOI-X (Heidari, Hebrard, et al in prep):

P (d)	40.36 ± 0.01
R (RJ)	0.91 ± 0.05
Mass (MJ)	1.07 ± 0.10

CHEOPS proposal has been submitted:

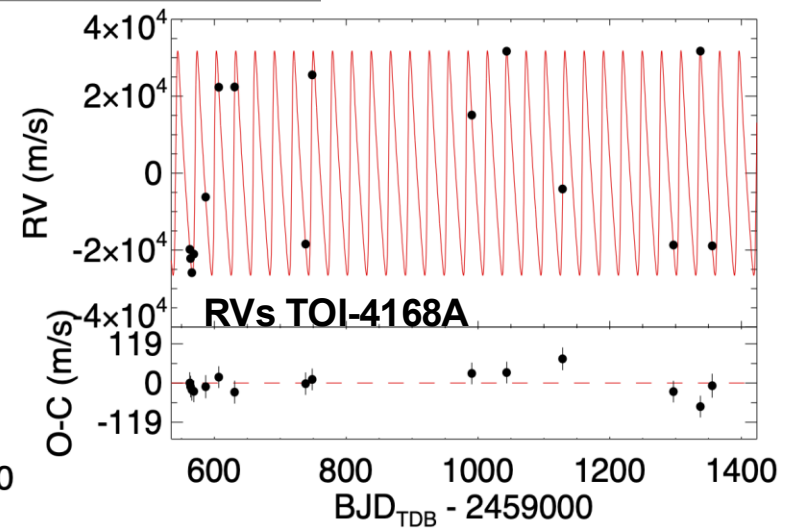
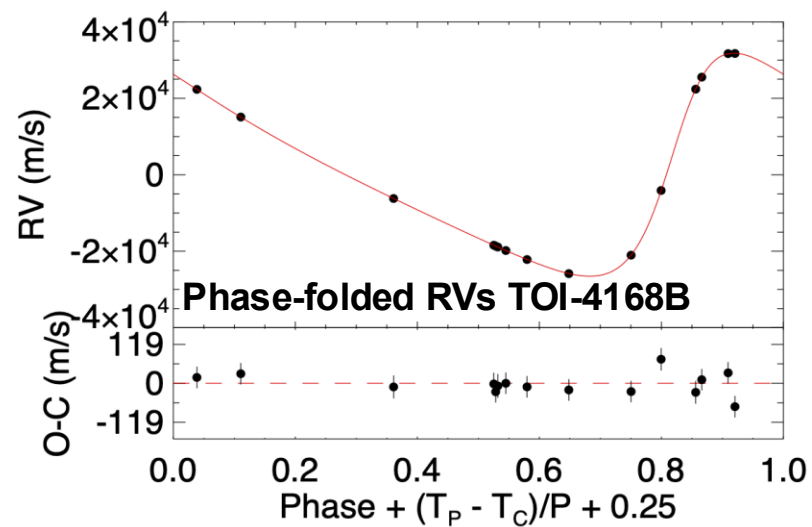
- To more precisely determine the planet period
- Reducing its uncertainty from approximately 2.3% (using TESS data alone) to around 0.03%
- $RM = 38 \pm 9$ m/s and possible to be measured using several ground based telescopes.



Top-left: SOPHIE RV time series. Top-right: TESS Sector 55 light curve. Middle-left: Phase-folded RV measurements. Middle-right: Phase-folded TESS sector 55 transit light curve. In all panels, the red curves show the best-fit median models obtained using *EXOFASTv2*, with residuals displayed beneath each plot. Bottom shows the TESS Sector 82 light curve, where the horizontal pink line indicates the predicted transit time based on the joint analysis of RV and photometric data of sector 55.

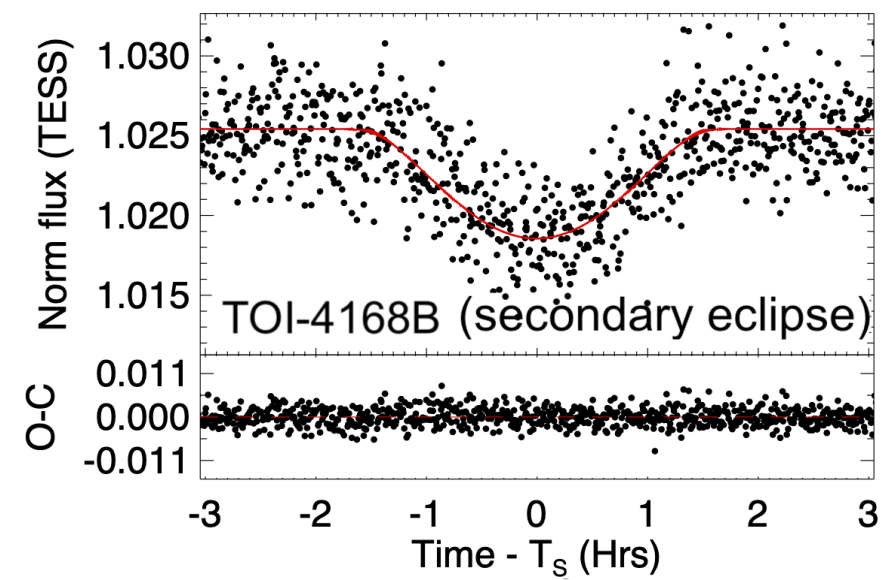
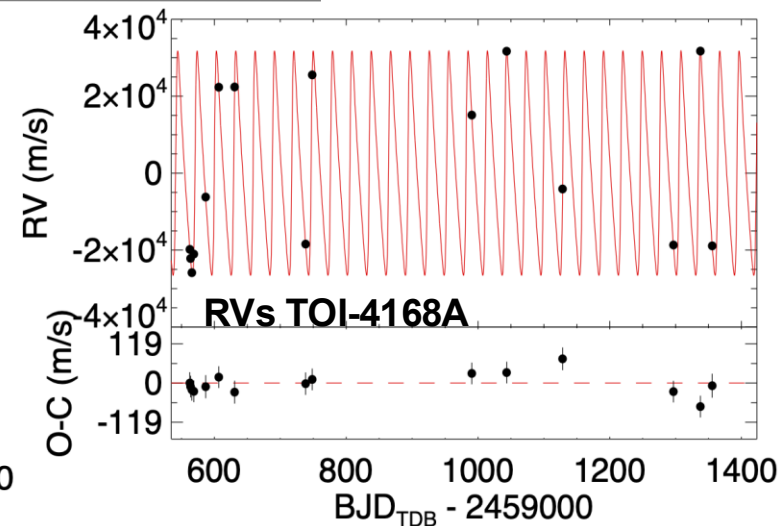
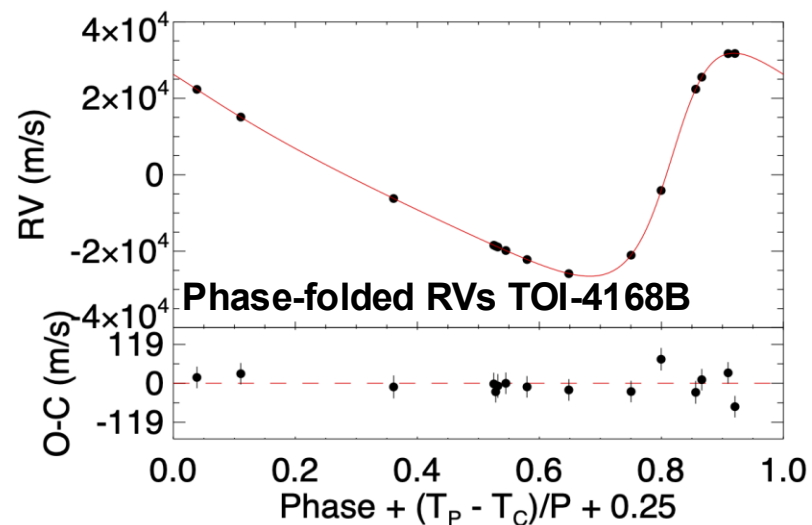
TOI-4168AB (Heidari, Hebrard, et al 2024):

RV curve exhibits an antiphase relation with the transit ephemeris observed by TESS, consistent instead with a secondary eclipse



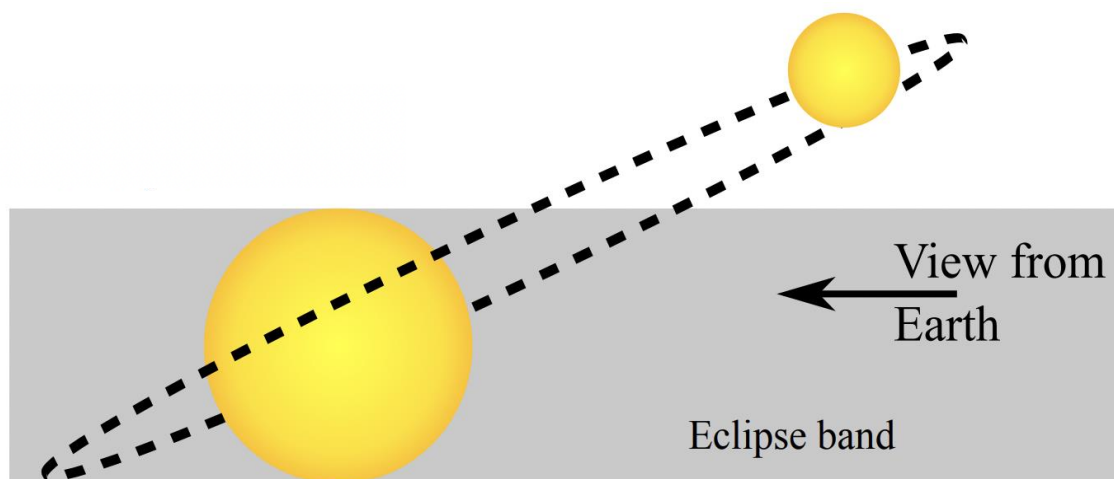
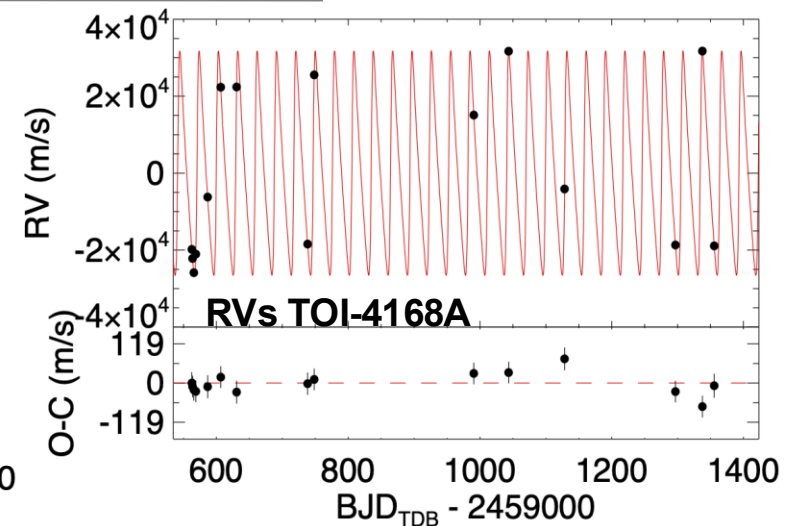
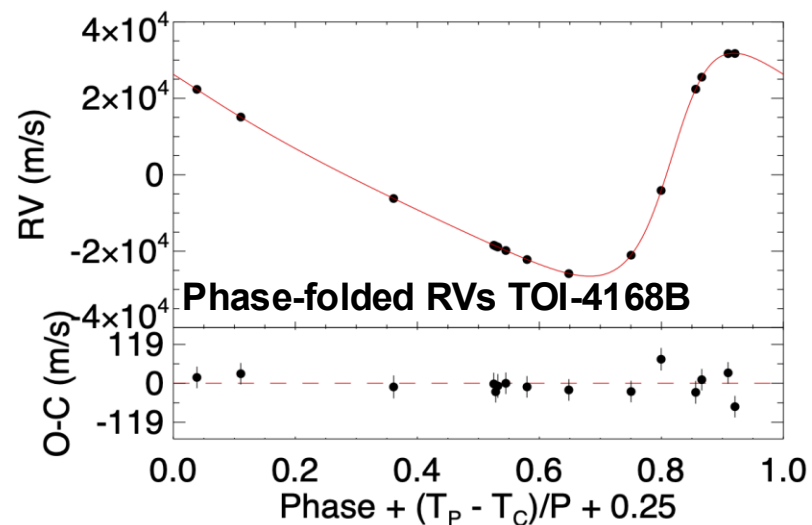
TOI-4168AB (Heidari, Hebrard, et al 2024):

RV curve exhibits an antiphase relation with the transit ephemeris observed by TESS, consistent instead with a secondary eclipse

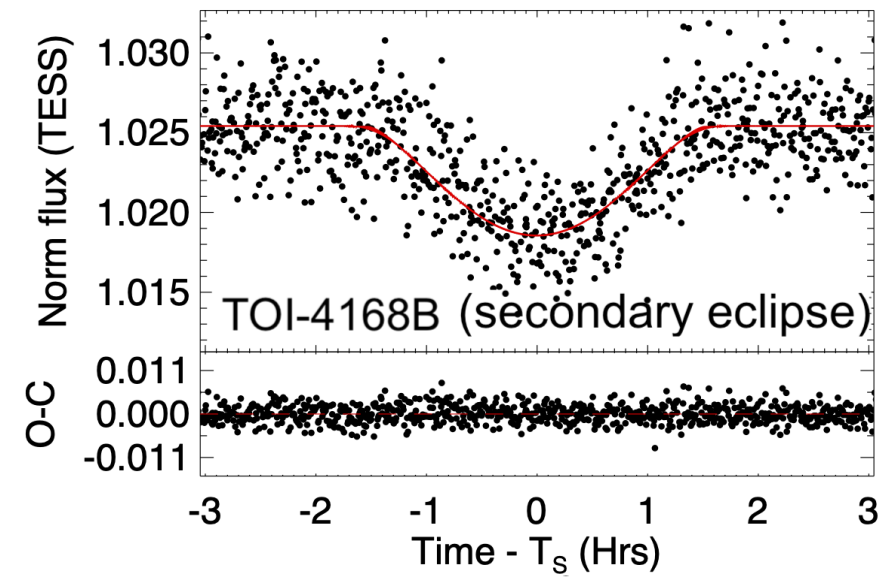


TOI-4168AB (Heidari, Hebrard, et al 2024):

RV curve exhibits an antiphase relation with the transit ephemeris observed by TESS, consistent instead with a secondary eclipse

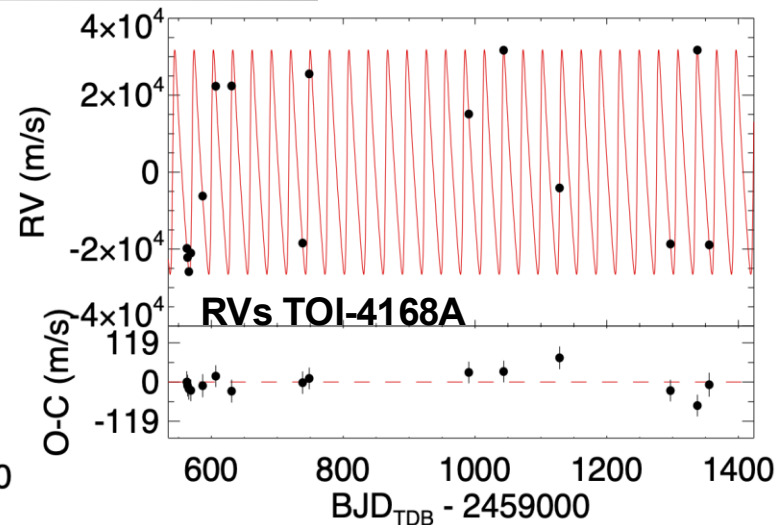
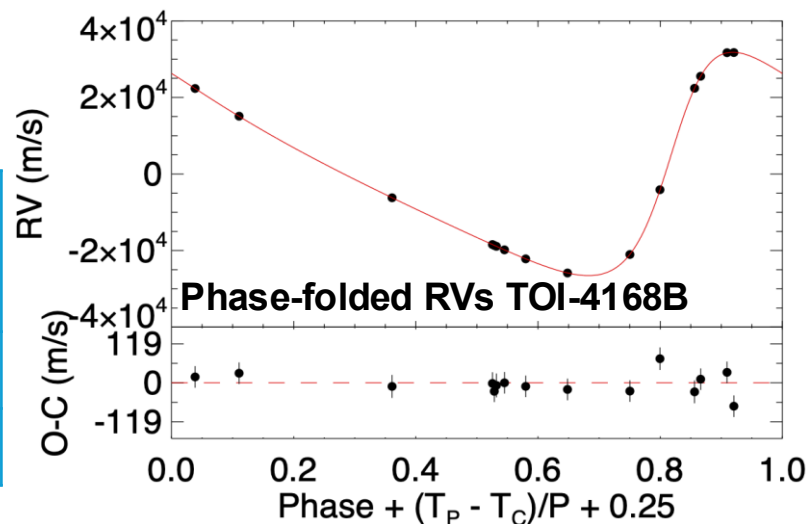


Sketch of the configuration where a binary only shows a secondary eclipse (Santerne+, 2013)

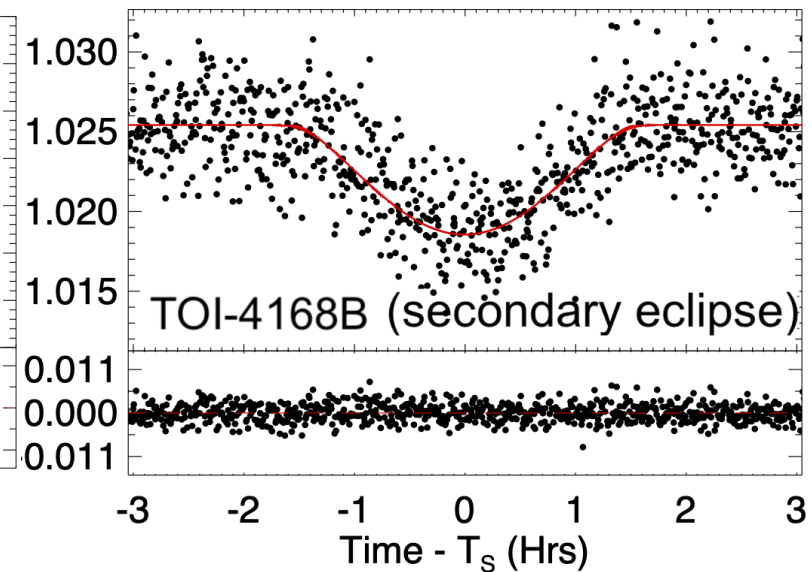
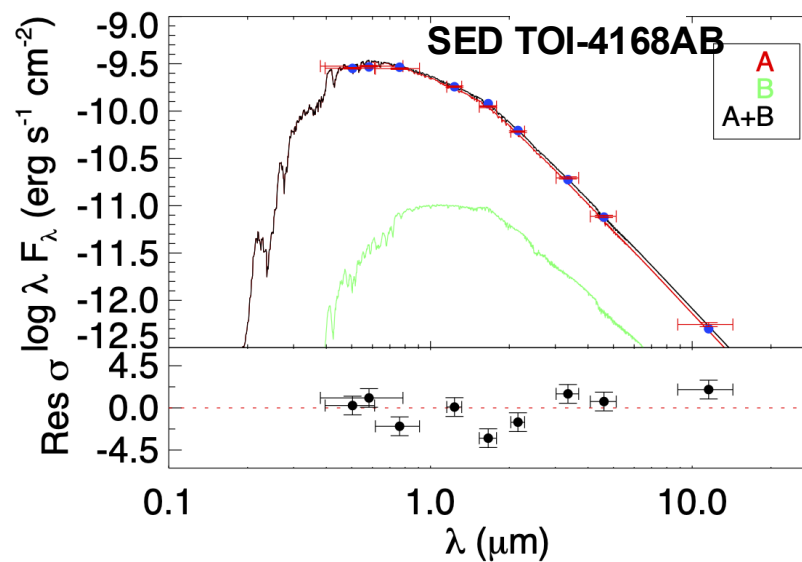


TOI-4168AB (Heidari, Hebrard, et al 2024):

Parameter	TOI-4168A	TOI-4168B
M_* (M_{sun})	1.02 ± 0.07	0.51 ± 0.02
R_* (R_{sun})	1.16 ± 0.05	0.48 ± 0.02



Period (d)	29.38167 ± 0.00005
e	0.4352 ± 0.0005
b (primary)	2.79 ± 0.07
b (secondary)	1.13 ± 0.03



Top-right: SOPHIE RV time series. Top-left: Phase-folded RV measurements. Bottom-left: TESS phase folded on secondary eclipse. Bottom-right: SED of TOI-4168AB. In all panels, the red curves show the best-fit median models obtained using EXOFASTv2, with residuals displayed beneath each plot.

Long-period planets are valuable targets for a variety of reasons, particularly for understanding planet formation and dynamical evolution.

TOI-2537 b & c ([Heidari, Hebrard, et al 2024](#)):

- TOI-2537 b has an orbital period of approximately 3 months and lies partially within the habitable zone.
- It exhibits strong TTVs, likely induced by the outer companion, planet c.
- Additional transit observations are required to refine the orbital parameters and improve our understanding of the system's architecture.

TOI-5110 b ([Heidari, Hebrard, et al 2024](#)):

- This planet is highly eccentric, with an eccentricity of $e \approx 0.75$.
- One possible explanation for this extreme eccentricity is the presence of an as-yet undetected low-mass planet on a shorter-period orbit.